จุฬาลงกรณ์มหาวิทยาลัย

ทุนวิจัย

กองทุนรัชดาภิเษกสมโภช

รายงานการวิจัย

การปรับปรุงสมบัติทางกายภาพของนาโนโพสิต ของพอลิโพรพิลีนและท่อนาโนคาร์บอน ด้วยการเติมพอลิเมอร์ชีวภาพ : การจำลองพลวัติเชิงโมเลกุล

โดย

ศาสตราจารย์ ดร.สุพจน์ หารหนองบัว

ตุลาคม 2563

กิตติกรรมประกาศ

โครงการนี้ได้รับทุนอุดหนุนการวิจัยจากจุฬาลงกรณ์มหาวิทยาลัย (This research is funded by Chulalongkorn University: CU_GR_62_11_23_05)

บทคัดย่อ

คาร์บอนนาโนฮอร์น (CNHs) สามารถใช้เป็นวัสดุในกระบวนการนำส่งยาสำหรับยารักษาโรคมะเร็ง อย่างไรก็ตาม CNH บริสุทธิ์มีคุณสมบัติที่เป็นข้อเสียต่อร่ายกายของมนุษย์ เช่น คุณสมบัติการละลายน้ำที่ต่ำ รวมไปถึงมีความเป็นพิษต่อระบบภายในร่างกายของมนุษย์ เพื่อแก้ปัญหาดังกล่าว การเพิ่มสารพอลิเมอร์ชีวภาพ เช่น ไคโตซาน (CS) และ เบต้าไซโครเดกตริน (βCD) เป็นวิธีการช่วยเพิ่มคุณสมบัติการละลายน้ำและลดความเป็นพิษต่อร่างกายมนุษย์ได้ ในการศึกษานี้ เราได้ออกแบบระบบนำส่งยาที่มีประสิทธิภาพเพื่อใช้ในการนำส่งยารักษาโรคมะเร็ง อย่าง doxorubicin (DOX) โดยทำการศึกษาการกักเก็บยารักษาโรคมะเร็ง DOX ภายในและภายนอกท่อ CNH โดยแต่ละระบบจะมีความแตกต่างกันที่สารพอลิเมอร์ชีวภาพที่เพิ่มเข้าไป ได้แก่ ระบบที่ประกอบด้วย CNH บริสุทธิ์ และยา DOX (CNH/DOX), ระบบที่ประกอบด้วย CNH ที่ถูกพันด้วยสาย CS ในลักษณะเกลียวและยา DOX (CS-f-CNH/DOX) และระบบที่ประกอบด้วย CNH ที่ถูกพันด้วย CS ในลักษณะเกลียวโดยมี 2,6-dimethyl-β-cyclodextrin (DMβCD ต่อบริเวณปลายสาย CS และยา DOX และแต่ละระบบจะถูกแยกโดยการโหลดยาภายในหรือภายนอกท่อ CNH โดยทุกระบบจะถูกศึกษาด้วยวิธีการจำลองพลวัตเชิงโมเลกุล (MD) ที่เหมือนกันและถูกคำนวณพลังงานเพื่อศึกษาการยึดจับของยากับโพลอเมอร์ต่าง ๆ ด้วยการคำนวณ MMPBSA จากการศึกษาพบว่าอันตรกิริยาระหว่างท่อ CNH กับยา DOX ที่อยู่ข้างในท่อ เกิดอันตรกิริยาที่แข็งแรงกว่าอันตรกิริยาระหว่างท่อ CNH กับยา DOX ที่อยู่ภายนอกท่อ นอกจากนี้ จากการศึกษาการเคลื่อนที่ของยาพบว่ายาจะเคลื่อนที่บริเวณพื้นผิวท่อส่วนกลางและปากท่อ CNH สำหรับยา DOX ที่อยู่บริเวณบนสาย CS พบว่ายามีการเคลื่อนที่ที่น้อยและสามารถเคลื่อนที่แทรกลงไปยังพื้นผิวของท่อที่ถูกล้อมด้วย CS ได้ จากผลการศึกษาสามารถสรุปได้ว่า CNH บริสุทธิ์และ CNH ที่ถูกเพิ่มสารชีวพอลิเมอร์สามารถใช้สำหรับการนำส่งได้ โดยยาสามารถโหลดเก็บยาได้ทั้งบริเวณพื้นผิวภายนอกและภายในท่อ

Carbon nanohorns (CNHs) are considered as promising drug carriers for cancer therapy. However, the pristine CNHs exhibit low solubility and dispersion in aqueous solution, and especially are high toxicity to our body. To solve such problems, the mixture of biocompatible polymers such as chitosan (CS) and β-cyclodextrin (βCD) with CNHs is rather promising. In this study, we modeled an effective delivery system of doxorubicin anticancer drug in complex with pristine CNH and functionalized CNH. To investigate the loading of anticancer drug, doxorubicin, we prepared an effective drug delivery system for delivery the drug, such as pristine carbon nanohorn system (CNH/DOX), chitosan functionalized CNH system (CS-f-CNH/DOX) and 2,6-dimethyl-β-cyclodextrin (DMBCD) on CS functionalized carbon nanohorn system (CS-f-CNH/DOX/CD). All atom molecular dynamics (MD) simulations were firstly carried out on all types of drug delivery system and then the binding free energy were performed by MMPBSA method. The binding of DOX inside and outside indicated that the binding between DOX and CNH is higher than that between DOX and CS. Moreover, the movement of drug inside and outside CNH surfaces suggest that DOXs can stably move around middle and edge of CNH while the DOXs on CS slightly move around initial CS residues. In conclusion, all data showed that the designed drug delivery systems of CNH and functionalized CNH can be served as drug carrier.

สารบัญ

บทนำ

ในปัจจุบันผู้คนส่วนใหญ่มีความกังวลเกี่ยวกับโรคมะเร็ง โดยโรคมะเร็งถูกระบุว่าเป็นสาเหตุการตายอันดับ 2 ของมนุษย์ในปี พ.ศ. 2561 สำหรับในประเทศไทยพบว่ามีประชากรเพศหญิงเป็นโรคมะเร็งเพิ่มขึ้นในทุก ๆ ปี อย่างไรก็ตาม ในปัจจุบันมียาบางชนิดถูกพัฒนาเพื่อรักษาโรคมะเร็ง โดยยา Doxorubicin (DOX; Adriamycin) ถูกระบุว่าเป็นยาที่มีประสิทธิภาพในการยับยั้งโรคมะเร็งหลายชนิด อย่างไรก็ตาม ยารักษาโรคมะเร็งไม่ได้ฆ่าเฉพาะเซลล์มะเร็งเท่านั้น โดยยารักษาโรคมะเร็งในกลุ่มนี้สามารถทำลายเซลล์ปกติในร่างการมนุษย์ได้ด้วย ทำให้เกิดผลข้างเคียงจากการใช้ยา เพื่อที่จะลดผลข้างเคียงดังกล่าว ระบบการนำส่งยา (drug delivery system) หรือ (DDS) จึงถูกนำมาประยุคใช้เพื่อนำส่งยาไปยังเซลล์เป้าหมายอย่างเฉพาะเจาะจง โดยไม่ให้ยาเข้าสู่เซลล์ปกติก่อนที่ยาจะถึงเซลล์เป้าหมายหรือเซลล์มะเร็ง

ปัจจุบันมีการศึกษาที่เกี่ยวข้องกับ DDS จำนวนมาก โดยมีการศึกษาสารและวัสดุชีวภาพหลายชนิดที่ถูกนำมาใช้ใน DDS ตัวอย่างเช่น liposome cyclodextrin lipid nanocapsules และวัสดุนาโนคาร์บอน (carbon nanomaterial) โดยหลักการแล้วสารหรือวัสดุที่สามารถใช้ในการนำส่งยา คือวัสดุที่สามารถกักเก็บยาได้จำนวนมากและเกิดอันตรกิริยาระหว่างโมเลกุลกับยาได้ดีและสามารถปลดปล่อยยาได้เมื่อยาเดินทางมาถึงเป้าหมายและไม่เป็นพิษต่อร่างกาย ตัวอย่างวัสดุที่ได้รับการศึกษาในปัจจุบันคือ carbon nanomaterial เช่น carbon nanotube (CNT) เป็นต้น อีกหนึ่งวัสดุที่น่าสนใจคือ carbon nanohorn (CNH) ซึ่งสามารถเกิดการรวมกลุ่มได้หลายแบบ เช่น petal-dahlia-like, dahlia-like, bud-like และ seed-like เป็นต้น อย่างไรก็ตาม CNT และ CNH มีคุณสมบัติที่เป็นข้อเสียต่อร่างกายที่เหมือนกัน ตัวอย่างเช่น มีค่าการละลายน้ำที่ต่ำและมีความเป็นพิษต่อร่างกายมนุษย์ สำหรับโพลิเมอร์ชนิดอื่น ๆ เช่น cyclodextrin (CD) ได้ถูกศึกษาเป็นจำนวนมาก โดย CD ที่นิยมในการศึกษาจะประกอบด้วยน้ำตาล glucoses จำนวน 6 ถึง 8 หน่วย โดยแยกออกเป็น α-, β- และ γ-CD ตามลำดับ โดย DMβCD เป็นอนุพันธ์ของ βCD ได้ถูกศึกษาเป็นพาหนะสำหรับการนำส่งยา DOX นอกจากนี้ βCD ยังสามารถคอนจูเกตกับ chitosan (CS) เพื่อเพิ่มปริมาณการกักเก็บยาได้ โดย CS เป็นไบโอพอลิเมอร์ ที่สามารถละลายน้ำได้ดี และมีคุณสมบัติการที่ดีเหมาะที่จะใช้ในกระบวนการนำส่งยา โดยก่อนหน้านี้ CNT ได้ถูกศึกษาคุณสมบัติในการนำส่งยา DOX ซึ่ง CNT สามารถนำส่งยาได้ดีเมื่ออยู่ในสภาวะ pH 7 (เป็นสภาวะของเซลล์ปกติ) ในงานวิจัยนี้ เป็นการศึกษาเพื่อหาโพลิเมอร์ชนิดใหม่ ๆ ที่มีคุณสมบัตินำส่งยาอย่าง CNH และรวมไปถึงการปรับปรุงคุณสมบัติที่เป็นข้อเสีย เช่น การละลายน้ำ และลดความเป็นพิษของ CNH ด้วยการเพิ่มโพลิเมอร์ชีวภาพอย่าง CS โดยทำการพันรอบ ๆ ท่อ CNH (CS-f-CNH) และเพิ่ม DMβCD บริเวณปลายสายของ CS (CS-f-CNH/CD) โดยมีวัตถุประสงค์ในการศึกษาดังนี้

1. ศึกษาระบบ CNH ที่ถูกเติมสารพอลิเมอร์ชีวภาพที่สามารถช่วยเพิ่มคุณสมบัติการละลายน้ำและลดความเป็นพิษ และสามารถยึดเกาะกับท่อ CNH ได้ดี
2. ศึกษาคุณสมบัติการนำส่งยา เช่น ศึกษาอันตรกิริยาระหว่างท่อ CNH บริสุทธิ์และ CNH ที่ถูกเติมด้วยพอลิเมอร์ชีวภาพและยารักษาโรคมะเร็ง DOX

เนื้อเรื่อง อภิปราย/วิจารณ์ผลการทดลอง

ได้ทำการวิจัยตามแผนในตาราง โดยรายละเอียดของวิธีการทดลอง ผลการทดลอง อภิปราย/วิจารณ์ผลการทดลอง ดังเอกสารแนบ (อยู่ในระหว่างเตรียมผลงานตีพิมพ์อีก 1 ฉบับ)

กิจกรรม	ผลผลิต
1. สร้างพารามิเตอร์ของท่อนาโนฮอร์น ไซโคลเด็กทรินซ์ ไคโตซาน และยาด็อกโซรูบิซินด้วยวิธีการคำนวณเชิงควอนตัม	ได้พารามิเตอร์ที่จำเป็นในการจำลองพลวัติเชิงโมเลกุล
2. สร้างโครงสร้างเริ่มต้นของสารประกอบเชิงซ้อนระหว่าง (i) ท่อนาโนฮอร์นกับยา (ii) ท่อนาโนฮอร์นพันด้วยไคโตซานกับยา (iii) ท่อนาโนฮอร์นพันด้วยไคโตซานและไซโคลเด็กทรินซ์กับยา	ได้โครงสร้างเริ่มต้นของระบบนำส่งยา 3 รูปแบบ
3. จำลองพลวัตเชิงโมเลกุลที่อุณหภูมิ 298 K เป็นเวลา 500 นาโนวินาที	ได้โครงสร้างที่เก็บได้ จากการคำนวณโดยวิธีการจำลองพลวัติเชิงโมเลกุลเป็นเวลา 500 นาโนวินาที
4.วิเคราะห์ชนิดของอันตรกิริยา สมบัติเชิงโครงสร้าง และกลไกการขนส่งยาด็อกโซรูบิซินจากระบบนำส่งยาแบบต่างๆ	ได้ข้อมูลพื้นฐานเชิงโมเลกุลที่สำคัญ ความเข้าใจถึงพฤติกรรมและยึดจับกันระหว่างยากับท่อนาโนฮอร์น ยากับไคโตซานที่พันรอบท่อนาโนฮอร์น และยากับไซโคลเด็กทรินซ์ที่ต่อกับไคโตซานที่พันรอบท่อนาโนฮอร์น
5. วิเคราะห์ข้อมูลเปรียบเทียบกับผลการทดลอง สรุปผล และเขียนผลงานเพื่อตีพิมพ์ในวารสารระดับนานาชาติ	ผลงานอยู่ในระหว่างเตรียมส่งตีพิมพ์อีก 1 ฉบับ

สรุปผลการวิจัย

ได้ผลการวิจัยอยู่ในระหว่างเตรียมผลงานตีพิมพ์ 1 ฉบับ ดังนี้

ชื่อบทความ The Use of Pristine and Chitosan Functionalized Carbon Nanohorn as Drug Carrier for Targeted Drug Delivery System in Cancer Therapy
ชื่อวารสาร Journal of Molecular Graphics and Modelling
High impact factor (ระดับ) โปรดระบุ 2.079

ภาคผนวก

The Use of Pristine and Chitosan Functionalized Carbon Nanohorn as Drug Carrier for Targeted Drug Delivery System in Cancer Therapy

Napat Kongtaworn[1], Bodee Nutho[2], Panupong Mahalapbutr[3], Nutpanai Ustagitavee[3], Chompoonut Rungnim[4], Supot Hannongbua[5] and Thanyada Rungrotmongkol[1,2*]

[1]Program in Bioinformatics and Computational Biology, Graduate School, Chulalongkorn University, Bangkok 10330, Thailand

[2]Center of Excellence in Computational Chemistry (CECC), Department of Chemistry, Faculty of Science, Chulalongkorn University, Bangkok 10330, Thailand

[3]Structural and Computational Biology Research Unit, Department of Biochemistry, Faculty of Science, Chulalongkorn University, Bangkok 10330, Thailand

[4]National Nanotechnology Center (NANOTEC), National Science and Technology Development Agency (NSTDA), Pathum Thani 12120, Thailand

[5]Center of Excellence in Computational Chemistry (CECC), Department of Chemistry, Faculty of Science, Chulalongkorn University, Bangkok 10330, Thailand; supot.h@chula.ac.th

[*]Corresponding authors. TR Fax: +66 2 218-5418; Tel: +66 2 218-5426

E-mail address: thanyada.r@chula.ac.th, chompoonut.run@nectec.or.th

ประวัตินักวิจัย

ชื่อ (ภาษาไทย) ธัญญดา รุ่งโรจน์มงคล

ชื่อ (ภาษาอังกฤษ) Thanyada Rungrotmongkol

วันเดือนปีเกิด 14 January1979

สถานที่เกิด Ratchaburi province

สถานภาพการสมรส -

ตำแหน่งปัจจุบัน Assistant Professor in Chemistry

ที่อยู่หน่วยงาน / โทรศัพท์ / โทรศัพท์เคลื่อนที่

Department of Biochemistry, Faculty of Science, Chulalongkorn University

254 Phayathai Rd., Patumwan, Bangkok, 10330, Thailand

E-mail address: thanyada.r@chula.ac.th, t.rungrotmongkol@gmail.com

Phone Number: +66-2218-5426

ประวัติการศึกษา

Year	Degree	Institute
2001	B.Sc. in Chemistry (with First Class Honors)	Kasetsart University
2006	Ph.D. in Physical Chemistry	Kasetsart University

ผลงานวิจัยเด่น เช่น วารสารวิชาการระดับนานาชาติ วารสารวิชาการระดับชาติ หนังสือ สิทธิบัตร (ในประเทศและต่างประเทศ)

1. **T. Rungrotmongkol**, S. Hannongbua* and A. J. Mulholland, Mechanistic study of HIV-1 reverse transcriptase at the active site based on QM/MM method, *Journal of Theoretical and Computational Chemistry* **2004**; 3(4): 491-500.
2. **T. Rungrotmongkol**, A. J. Mulholland and S. Hannongbua*, Active site dynamics and combined quantum mechanics/ molecular mechanics (QM/ MM) modelling of a HIV- 1 reverse transcriptase/DNA/dTTP complex, *Journal of molecular graphics and modelling* **2007**; 26(1): 1-13.
3. M. Malaisree, **T. Rungrotmongkol**, P. Decha, P. Intharathep, O. Aruksakunwong, and S. Hannongbua*, Understanding of known drug-target interactions in the catalytic pocket of neuraminidase subtype N1, *Proteins* **2008**; 71(4): 1908-191
4. P. Decha, **T. Rungrotmongkol**, P. Intharathep, M. Malaisree, O. Aruksakunwong, C. Laohpongspaisan, V. Parasuk, P.Sompornpisut, S. Pianwanit, S. Kokpol and S. Hannongbua*, Source of high pathogenicity of an avian influenza virus H5N1: Why H5 is better cleaved by furin, *Biophysical Journal* **2008**; 95(1): 128-134.
5. V. Nukoolkarn, S. Saen-oon, **T. Rungrotmongkol**, S. Hannongbua, K. Ingkaninan, K. Suwanborirux*, Petrosamine, a potent anticholinesterase pyridoacridine alkaloid from a Thai marine sponge Petrosia n. sp., *Bioorganic & Medicinal Chemistry* **2008**; 16(13): 6560-6567.
6. **T. Rungrotmongkol**, P. Decha, M. Malaisree, P. Sompornpisut, and S. Hannongbua*, Comment on ''Cleavage mechanism of the H5N1 hemagglutinin by trypsin and furin'' [Amino Acids 2008, January 31, Doi: 10.1007=s00726-007-0611-3], *Amino Acids* **2008**; 35: 511-512.

7. P. Intharathep, C. Laohpongspaisan, **T. Rungrotmongkol**, A. Loisruangsin, M. Malaisree, P. Decha, O. Aruksakunwong, K. Chuenpennit, N. Kaiyawet, P. Sompornpisut, S. Pianwanit, and S. Hannongbua*, How amantadine and rimantadine inhibit proton transport in the M2 protein channel, *Journal of Molecular Graphics and Modelling* **2008**; 27(3): 342-348.
8. **T. Rungrotmongkol**, V. Frecer, W. De-Eknamkul, S. Hannongbua, and S. Miertus*, Design and in silico screening of combinatorial library of oseltamivir analogs inhibiting neuraminidase of avian influenza virus H5N1. *Antiviral Research* **2009**; 82(1):51-8.
9. **T. Rungrotmongkol**, M. Malaisree, T. Udommaneethanakit and S. Hannongbua*, Comment on "Another look at the molecular mechanism of the resistance of H5N1 influenza A virus neuraminidase (NA) to oseltamivir (OTV)". *Biophysical Chemistry* **2009**; 141: 131-132.
10. C. Laohpongspaisan, **T. Rungrotmongkol**, P. Intharathep, M. Malaisree, P. Decha, O. Aruksakunwong, P. Sompornpisut, S. Hannongbua*, Why amantadine loses its function in influenza M2 mutants: MD simulations. *Journal of Chemical Information and Modeling* **2009**; 49(4):847-52.
11. **T. Rungrotmongkol**, P. Decha, P. Sompornpisut, M. Malaisree, P. Intharathep, N. Nunthaboot, T. Udommaneethanakit, O. Aruksakunwong, and S. Hannongbua*, Combined QM/MM mechanistic study of the acylation process in furin complexed with the H5N1 avian influenza virus hemagglutinin's cleavage site. *Proteins: Structure, Function, and Bioinformatics* **2009**; 76(1): 62-71
12. **T. Rungrotmongkol**, P. Intharathep, M. Malaisree, N. Nunthaboot, N. Kaiyawet, P. Sompornpisut, S. Payungporn, Y. Poovorawan, and S. Hannongbua*, Susceptibility of antiviral drugs against 2009 influenza A (H1N1) virus. *Biochemical and Biophysical Research Communications* **2009**; 385(3):390-4.
13. M. Malaisree[a], **T. Rungrotmongkol**[a], N. Nunthaboot, O. Aruksakunwong, P. Intharathep, P. Decha, P. Sompornpisut and S. Hannongbua*, Source of Oseltamivir Resistance in Avian Influenza H5N1 Virus with the H274Y Mutation. *Amino Acids* **2009**; 37(4):725–732.
14. T. Udommaneethanakit, **T. Rungrotmongkol**, U. Bren, V. Frecer and S. Miertus*, Dynamic Behavior of Avian Influenza A Virus Neuraminidase Subtype H5N1 in Complex with Oseltamivir, Zanamivir, Peramivir, and their Phosphonate Analogues, *Journal of Chemical Information and Modeling* **2009**; 49(10):2323–2332.
15. **T. Rungrotmongkol**, T. Udommaneethanakit, M. Malaisree, N. Nunthaboot, P. Intharathep, P. Sompornpisut and S. Hannongbua*, How does each substituent functional group of oseltamivir lose its activity against virulent H5N1 influenza mutants? *Biophysical Chemistry* **2009**; 145(1):29–36.
16. **T. Rungrotmongkol**, T. Udommaneethanakit, V. Frecer, and S. Miertus, Combinatorial design of avian influenza neuraminidase inhibitors containing pyrrolidine core with a reduced susceptibility to viral drug resistance, *Combinatorial Chemistry & High Throughput Screening* **2010**; 13(3):268-77.
17. N. Nunthaboot, **T. Rungrotmongkol**, M. Malaisree, P. Decha, N. Kaiyawet, P. Intharathep, P. Sompornpisut, Y. Poovorawan and S. Hannongbua*, Molecular insights into human receptor binding to 2009 H1N1 influenza A hemagglutinin, *Monatshefte fur Chemie - Chemical Monthly* **2010**; 141(7):801-807.

18. **T. Rungrotmongkol**[a], M. Malaisree[a], N. Nunthaboot, P. Sompornpisut, and S. Hannongbua*, Molecular prediction of oseltamivir efficiency against probable influenza A (H1N1-2009) mutants: Molecular modelling approach, *Amino Acids* **2010**; 39(2):393-398.
19. S. Phongphanphanee, **T. Rungrotmongkol**, N. Yoshida, S. Hannongbua, F. Hirata*, Proton transport through the influenza A M2 channel: 3D-RISM study, *Journal of American Chemical Society* **2010**; 132(28):9782-9788.
20. N. Nunthaboot, **T. Rungrotmongkol**, M. Malaisree, N. Kaiyawet, P. Decha, P. Sompornpisut, and S. Hannongbua*, Evolution of human receptor binding affinity of h1n1 hemagglutinins from 1918 to 2009 pandemic influenza A virus, *Journal of Chemical Information and Modeling* **2010**;50(8):1410-1417.
21. **T. Rungrotmongkol***, N. Nunthaboot, M. Malaisree, N. Kaiyawet, P. Yotmanee, A. Meepraset and S. Hannongbua, Molecular Insight into the Specific Binding of ADP-ribose to the nsP3 Macro Domains of Chikungunya and Venezuelan Equine Encephalitis Viruses: Molecular Dynamics Simulations and Free Energy Calculations, *Journal of Molecular Graphics and Modelling* **2010**;29(3):347–353.
22. U. Arsawang, O. Saengsawang, **T. Rungrotmongkol**, P. Sornmee, K. Wittayanarakul, T. Remsungnen and S. Hannongbua*, How do carbon nanotubes serve as carriers for gemcitabine transport in drug delivery system? *Journal of Molecular Graphics and Modelling* **2011**;29(5):591–596.
23. P. Intharathep, **T. Rungrotmongkol**, P. Decha, N. Nunthaboot, N. Kaiyawet, T. Kerdcharoen, P. Sompornpisut, and S. Hannongbua*, Evaluating how rimantadines control the proton gating of the Influenza A M2-proton port via allosteric binding outside of the M2-channel: MD simulations, *Journal of Enzyme Inhibition and Medicinal Chemistry* **2011**; 26(2):162-168.
24. **T. Rungrotmongkol**, U. Arsawang, C. Iamsamai, A. Vongachariya, S. Dubas, U. Ruktanonchai, A. Soottitantawat and S. Hannongbua*, Increase dispersion and solubility of carbon nanotubes noncovalently modified by the polysaccharide biopolymer, chitosan: MD simulations, *Chemical Physics Letter* **2011**;507(1-3):134–137.
25. **T. Rungrotmongkol**[a], P. Yotmanee[a], N. Nunthaboot[a] and S. Hannongbua*, Computational studies of influenza A virus at three important targets: hemagglutinin, neuraminidase and M2 protein, *Current Pharmaceutical Design* **2011**;17(17):1720-1739. (review article)
26. P. Sornmee, **T. Rungrotmongkol**, O. Saengsawang, U. Arsawang, T. Remsungnen and S. Hannongbua*, Understanding the molecular properties of doxorubicin filling inside and wrapping outside single-walled carbon nanotubes, *Journal of Computational and Theoretical Nanosciencs* **2011**;8(8):1385-1391.
27. J. Kongkamnerd, L. Cappelletti, A. Prandi, P. Seneci*, **T. Rungrotmongkol**, N. Jongaroonngamsang, P. Rojsitthisak, V. Frecer*, A. Milani, G. Cattoli, C. Terregino, I. Capua, L. Beneduce, A. Gallotta, P. Pengo, G. Fassina, S. Miertus, W. De-Eknamkul*, Synthesis and in vitro study of novel neuraminidase inhibitors against avian influenza virus, *Bioorganic & Medicinal Chemistry* **2012**;20(6): 2152–2157
28. P. Kongsune, **T. Rungrotmongkol**, N. Nunthaboot, P. Yotmanee, P. Sompornpisut, Y. Poovorawan, P. Wolschann and S. Hannongbua*, Molecular insights into the binding affinity and specificity of the

hemagglutinin cleavage loop from four highly pathogenic H5N1 isolates towards the proprotein convertase furin, *Monatshefte fur Chemie - Chemical Monthly* **2012**;143(5):853–860.

29. A. Meeprasert, W. Khuntawee, K. Kamlungsua, N. Nunthaboot, **T. Rungrotmongkol***, S. Hannongbua, Binding pattern of the long acting neuraminidase inhibitor laninamivir toward influenza A subtypes H5N1 and pandemic H1N1, *Journal of Molecular Graphics and Modeling* **2012**;38: 148-154.
30. C. Rungnim, U, Arsawang, **T. Rungrotmongkol***, S Hannongbua, Molecular dynamics properties of varying amounts of the anticancer drug gemcitabine inside an open-ended single-walled carbon nanotube, *Chemical Physics Letter* **2012;** 550: 99-103.
31. A. Vongachariya, C. Iamsamai, O. Saengsawang, **T. Rungrotmongkol**, S. Dubas, V. Parasuk and S. Hannongbua*, The suface curvature effect of single-walled carbon nanotube on its cation-π interaction with monovalent cations, *Journal of Computational and Theoretical Nanosciencs* **2012;** 9(12), 2107-2112.
32. W. Khuntawee, **T. Rungrotmongkol*** and S. Hannongbua. Molecular Dynamic Behavior and Binding Affinity of Flavonoid Analogues to the Cyclin Dependent Kinase 6/cyclin D Complex, *Journal of Chemical Information and Modeling* **2012**;52:76–83.
33. C. Rungnim, T. Rungrotmongkol, S. Hannongbua*, H. Okumura, Replica exchange molecular dynamics simulation of chitosan for drug delivery system based on carbon nanotube, *Journal of Molecular Graphics and Modeling* **2013;** 39: 183-192.
34. N. Kaiyawet, **T. Rungrotmongkol*** and S. Hannongbua, Probable polybasic residues inserted into the cleavage site of the highly pathogenic avian influenza A/H5N1 hemagglutinin: speculation of the next outbreak in humans, *International Journal of Quantum Chemistry* **2013;** 113(4), 569–573.
35. P. Maitarad, D. Zhang*, R. Gao, L. Shi*, H. Li, L. Huang, **T. Rungrotmongkol**, J. Zhang, Combination of experimental and theoretical investigations of $MnO_x/Ce_{0.9}Zr_{0.1}O_2$ nanorods for selective catalytic reduction of NO with ammonia, *The Journal of Physical Chemistry C*, **2013**; 117(19): 9999–10006.
36. R. Gao, D. Zhang*, P. Maitarad, L. Shi*, **T. Rungrotmongkol**, H. Li, J. Zhang, W. Cao, Morphology-dependent properties of MnO_x/ZrO_2–CeO_2 nanostructures for the selective catalytic reduction of NO with NH3, *The Journal of Physical Chemistry C*, **2013**; 117 (20), 10502–1051.
37. N. Nunthaboot[a], T **Rungrotmongkol**[a], O. Aruksakunwong[a], S. Hannongbua*, Effects of protonation state of catalytic residues and ligands upon binding and recognition in targeted proteins of HIV-1 and influenza viruses, *Current Pharmaceutical Design* **2013;** 19(23), 4276-4290. (review article)
38. N. Kaiyawet, **T. Rungrotmongkol**, S. Hannongbua*, Effect of halogen substitutions on dUMP to stability of thymidylate synthase/dUMP/mTHF ternary complex using molecular dynamics simulation, *Journal of Chemical Information and Modeling*, **2013;** 53 (6), 1315–1323
39. **T. Rungrotmongkol**, A.J. Mulholland, S. Hannongbua*, QM/MM simulations indicate that Asp185 is the likely catalytic base in the enzymatic reaction of HIV-1 reverse transcriptase, *Medicinal Chemistry Communications*, 2014; 5(5): 593-596.
40. W. Sangpheak, W. Khuntawee, P. Wolschann, P. Pongsawasdi, **T. Rungrotmongkol***, Enhanced stability of naringenin/2,6-dimethyl β-cyclodextrin inclusion complex: Molecular dynamics and free

energy calculations based on MM- and QMPBSA/GBSA, *Journal of Molecular Graphics and Modeling,* **2014;** 50: 10–15.

41. A. Meeprasert, **T. Rungrotmongkol**, M.S. Li*, S Hannongbua*, In Silico screening for potent inhibitors against the NS3/4A protease of hepatitis C virus, *Current Pharmaceutical Design*, **2014;** 20(21), 3465-3477.
42. A. Meeprasert, S. Hannongbua, **T. Rungrotmongkol***, Key Binding and Susceptibility of NS3/4A Serine Protease Inhibitors against Hepatitis C Virus, *Journal of Chemical Information and Modeling*, **2014,** 54(4): 1208-17.
43. P. Maitarad, J. Han, D. Zhanga*,L. Shi, S. Namuangruk, **T. Rungrotmongkol**, Structure-Activity Relationships of NiO on CeO_2 Nanorods for Selective Catalytic Reduction of NO with NH_3: Experimental and DFT Studies, *The Journal of Physical Chemistry C*, **2014**; 118 (18), 9612–9620.
44. B. Nutho, W. Khuntawee, C. Rungnim, P. Pongsawasdi, P. Wolschann, A. Karpfen, N. Kungwan, **T. Rungrotmongkol***, Binding mode and free energy prediction of fisetin/β-cyclodextrin inclusion complex, *Beilstein Journal of Organic Chemistry*, **2014;** 10, 2789–2799.
45. T. Udommaneethanakit, **T. Rungrotmongkol**, V. Frecer, M. Stanislav, U. Bren*, Drugs against Avian Influenza A Virus: Design of Novel Sulfonate Inhibitors of Neuraminidase N1, *Current* Pharmaceutical Design, **2014**; 20(21):3478-87.
46. A. Suksuwan, L. Lomlim, **T. Rungrotmongkol**, T. Nakpheng, F.L. Dickert, R. Suedee*, The Composite Nanomaterials containing (R)-Thalidomide-Molecularly Imprinted Polymers as a Recognition System for Enantioselective- Controlled Release and Targeted Drug Delivery, *Journal of Applied Polymer Science*, **2015**; 132 (18): no.41930
47. M. Ratanasak, **T. Rungrotmongkol**, O. Saengsawang, S. Hannongbua, V. Parasuk, Towards the design of new electron donors for Ziegler-Natta catalyzed propylene polymerization using QSPR modeling. *Polymer (United Kingdom)* **2015**; 56, 340-345.
48. N. Kaiyawet, R. Lonsdale, **T. Rungrotmongkol**, A. Mulholland, S. Hannongbua*, High-Level QM/MM Calculations Support the Concerted Mechanism for Michael Addition and Covalent Complex Formation in Thymidylate Synthase, *Journal of Chemical Theory and Computation*, **2015**; 11 (2), 713–722.
49. S. Sirikataramas*, A. Meeprasert, **T. Rungrotmongkol**, H. Fuji, T. Hoshino, M. Yamazaki, K. Saito*, Structural insight of DNA topoisomerases I from camptothecin-producing plants revealed by molecular dynamics simulations, *Phytochemistry*, **2015**; 113:50-6.
50. P. Yotmanee, **T. Rungrotmongkol**, K. Wichapong, S. B. Choi, H. A. Wahab*, N. Kungwan, S. Hannongbua*, Binding specificity of polypeptide substrates in NS2B/NS3pro serine protease of dengue virus type 2: A molecular dynamics Study, *Journal of Molecular Graphics and Modeling* **2015**; 60, 24-33.
51. S. Kongkaew, P. Yotmanee, **T. Rungrotmongkol,** N. Kaiyawet, A. Meeprasert, T. Kaburaki, H. Noguchi, F. Takeuchi, N. Kungwan, S. Hannongbua*, Molecular Dynamics Simulation Reveals the Selective Binding of Human Leukocyte Antigen Alleles Associated with Behçet's Disease, PLoS One, **2015**; 10(9).

52. W. Khuntawee, P. Wolschann, **T. Rungrotmongkol***, J. Wong-ekkabut*, S Hannongbua, Molecular dynamics simulations of the interaction of Beta cyclodextrin with a lipid bilayer, *Journal of Chemical Information and Modeling*, **2015**, 55(9): 1894-1902.

53. C. Rungnim, S. Phunpee, M. Kunaseth, S. Namuangruk, K. Rungsardthong, **T. Rungrotmongkol***, U. Ruktanonchai*, Co-solvation effect on the binding mode of the α-mangostin/β-cyclodextrin inclusion complex, *Beilstein Journal of Organic Chemistry*, **2015**; 11, 2306–2317.

54. W. Sangpheak, J. Kicuntod, R. Schuster, **T. Rungrotmongkol**, P. Wolschann, N. Kuawan, H. Viernstein, M. Mueller*, P. Pongsawasdi*, Physical properties and biological activities of hesperetin and naringenin in complex with methylated β-cyclodextrin, *Beilstein Journal of Organic Chemistry*, **2015**; 11, 2763–2773.

55. J. Phanich, **T. Rungrotmongkol***, D. Sindhikara, S. Phongphanphanee, N. Yoshida, F. Hirata,* N. Kungwan, S. Hannongbua, A 3D-RISM/RISM study of the oseltamivir binding efficiency with the wild-type and resistance-associated mutant forms of the viral influenza B neuraminidase, *Protein Science*, **2016;** 25(1), 147-158.

56. A. Meeprasert, S. Hannongbua, N. Kungwan, **T. Rungrotmongkol***, Effect of D168V Mutation in NS3/4A HCV Protease on Susceptibilities of Faldaprevir and Danoprevir, *Molecular BioSystems*, **2016**, 12(12):3666-3673.

57. J. Kicuntod, W. Khuntawee, P. Wolschann, P. Pongsawasdi, N. Kuawan, **T. Rungrotmongkol*** Inclusion complexation of pinostrobin with various cyclodextrin derivatives, *Journal of Molecular Graphics and Modelling*, **2016**; 63, 91–98.

58. C. Rungnim, R. Chanajaree, **T. Rungrotmongkol**, S. Hannongbua, N. Kungwan, P. Wolschann, A. Karpfen*, V. Parasuk*, How strong is the edge effect in the adsorption of anticancer drugs on a graphene cluster?, *Journal of Molecular Modeling*, **2016**; 22(4)

59. W. Khuntawee, **T. Rungrotmongkol**, P. Wolschann, P. Pongsawasdi, N. Kungwan, H. Okumura*, S. Hannongbua* , Conformation study of ε-cyclodextrin: Replica exchange molecular dynamics simulations, *Carbohydrate Polymer*, **2016**, 141; 99–105.

60. N. Schaduangrat, J. Phanich, T. **Rungrotmongkol**, H. Lerdsamran, P. Puthavathana, S. Ubol*, The significance of naturally occurring neuraminidase quasispecies of H5N1 avian influenza virus on resistance to oseltamivir: a point of concern, *Journal of General Virology*, **2016**; 97(6):1311-23.

61. W. Karnsomwan, **T. Rungrotmongkol**, W. De-Eknamkul, S. Chamni*, *In silico* structural prediction of human steroid 5α-reductase Type II, *Med. Chem. Res.* **2016**; 25(6), 1049-1056.

62. R. Daengngern, C. Prommin; T. **Rungrotmongkol**, V. Promarak, P. Wolschann, N. Kungwan*, Theoretical investigation of 2-(iminomethyl)phenol in the gas phase as a prototype of ultrafast excited-state intramolecular proton transfer, *Chemical Physics Letters*, **2016**; 657, 113-118.

63. C. Rungnim, **T. Rungrotmongkol***, N. Kungwan, S. Hannongbua, Protein-protein interactions between SWCNT/chitosan/EGF and EGF receptor: A model of drug delivery system, *Journal of Biomolecular Structure & Dynamics*, **2016**, 34(9):1919-1929.

64. J. Phanich, **T. Rungrotmongkol***, N. Kungwan, S. Hannongbua*, Role of R292K mutation in influenza H7N9 neuraminidase toward oseltamivir susceptibility: MD and MM/PB(GB)SA study, *Journal of Computer-Aided Molecular Design*, 2016, 30(10), 917-926

65. S. Tantong, O. Pringsulaka, K. Weerawanich, A. Meeprasert, **T. Rungrotmongkol**, R. Sarnthima, S. Roytrakul, S. Sirikantaramas. Two novel antimicrobial defensins from rice identified by gene coexpression network analyses. *Peptides*, **2016**, 84, 7–16.

66. F.N. Sabri, H. Monajemi, S.M. Zain, P.S. Wai, **T. Rungrotmongkol**, V.S. Lee, Molecular conformation and UV–visible absorption spectrum of emeraldine salt polyaniline as a hydrazine sensor, *Integrated Ferroelectrics*, **2016**, 175(1): 202-210.

67. C. Rungnim, **T. Rungrotmongkol**, R. Poo-arporn*, pH-controlled doxorubicin anticancer loading and release from carbon nanotube noncovalently modified by chitosan: MD simulations, *Journal of Molecular Graphics and Modelling*, **2016**, 70, 70-76.

68. V.T. Phuong, T. Chokbunpiam*, S. Fritzsche, T. Remsungnen, **T. Rungrotmongkol**, C. Chmelik, J. Caro, S. Hannongbua*, Methane in Zeolitic Imidazolate Framework ZIF-90: Adsorption and Diffusion by Molecular Dynamics and Gibbs Ensemble Monte Carlo, *Microporous & Mesoporous Materials*, **2016**, 235, 69–77.

69. W. Jetsadawisut, B. Nutho, A. Meeprasert, **T. Rungrotmongkol,*** N. Kungwan, P. Wolschann, S. Hannongbua*, Susceptibility of inhibitors against 3C Protease of Coxsackievirus A16 and Enterovirus A71 Causing Hand, Foot and Mouth Disease: A Molecular Dynamics Study, *Biophysical Chemistry*, **2016**, 219, 9-16.

70. P. Wongpituk, B. Nutho, W. Panman, N. Kungwan, P. Wolschann, **T. Rungrotmongkol*** , N. Nunthaboot* , Structural dynamics and binding free energy of neral- cyclodextrins inclusion complexes: Molecular dynamics simulation, *Molecular Simulation*, **2017**, 43(13–16), 1356–1363

71. W. Karnsomwan, P. Netcharonensirisuk, **T. Rungrotmongkol**, W. De-Eknamkul, S. Chamni*, Synthesis, Biological Evaluation and Molecular Docking of Avicequinone C Analogues as Potential Steroid 5α-Reductase Inhibitors, *Chemical & Pharmaceutical Bulletin*, **2017**, 65(3): 253-260.

72. D. Saeloh, M. Wenzel, **T. Rungrotmongkol**, L. Hamoen, S. Voravuthikunchai, V. Tipmanee*, Effects of rhodomyrtone on Gram-positive bacterial tubulin homologue FtsZ, *Peer J.*, **2017**, 2;5:e2962.

73. B. Nutho, N. Nunthaboot*, P. Wolschann, N. Kungwan, T. **Rungrotmongkol***, Metadynamics supports molecular dynamics simulation-based binding affinities of eucalyptol and beta-cyclodextrins inclusion complexes, *RSC Advances*, **2017**, 7(80), 50899-50911.

74. S. Thompho, **T. Rungrotmongkol**, Oraphan Saengsawang, S. Hannongbua*, A Computational Study of Adsorption of Divalent Metal Ions on Graphene Oxide, *Songklanakarin Journal of Science and Technology*, **2017**, 39(6):773-778

75. W. Khuntawee, M. Kunaseth*, C. Rungnim, S. Intagorn, P. Wolschann, N. Kungwan, **T. Rungrotmongkol***, S. Hannongbua, Comparison of Implicit and Explicit Solvation Models for *Iota*-Cyclodextrin Conformation Analysis from Replica Exchange Molecular Dynamics, *Journal of Chemical Information and Modeling*, **2017**, 57 (4): 778-786.

76. B. Nutho, A. Meeprasert, M. Chulapa, N. Kungwan, **T. Rungrotmongkol***, Screening of Hepatitis C NS5B polymerase Inhibitors Containing Benzothiadiazine Core: A Steered Molecular Dynamics, *Journal of Biomolecular Structure & Dynamics,* **2017**; 35(8): 1743-1757.
77. S. Kruawan, M. Ratanasak, R. Chanajaree, T. **Rungrotmongkol**, O. Saengsawang, V. Parasuk, N. Kungwan, S. Hannongbua*, Ethylene insertion in the presence of new alkoxysilane electron donors for ziegler-natta catalyzed polyethylene, *Computational and Theoretical Chemistry*, **2017**, 1112: 10-19.
78. S. Raza, G. Sanober, T. **Rungrotmongkol**, S.S. Azam*, The Vitality of Swivel Domain Motion in Performance of Enzyme I of Phosphotransferase System; A Comprehensive Molecular Dynamic Study, *Journal of Molecular Liquids*, **2017**, 242: 1184-1198.
79. P. Mahalapbutr, P. Chusuth, N. Kungwan, W. Chavasiri, P. Wolschann, **T. Rungrotmongkol***, Molecular recognition of naphthoquinone-containing compounds against human DNA topoisomerase IIα ATPase domain: A molecular modeling study, *Journal of Molecular Liquids*, **2017**, 247, 374-385.
80. K. Nusai*, P. Doungdee, **T. Rungrotmongkol**, Study of drug likeness of praziquantel derivatives for the inhibition of thioredoxin peroxidase and aspartic protease in opisthorchis viverrini by molecular docking method, *KMITL Sci. Tech. J.*, **2017**, 17(1): Jan.-Jun.
81. W. Panman, B. Nutho, S. Chamni, S. Dokmaisrijan, N. Kungwan, T. **Rungrotmongkol***, Computational Screening of Fatty Acid Synthase Inhibitors Against Thioesterase Domain, *Journal of Biomolecular Structure and Dynamics* **2018**, 36(15), 4114-4125
82. P. Mahalapbutr, B. Nutho, P. Wolschann, N. Kungwan, T. **Rungrotmongkol***, Molecular Insights into Inclusion Complexes of Mansonone E and H Enantiomers with various β-cyclodextrins, *Journal of Molecular Graphics and Modeling*, **2018**, 79, 72-80
83. N. Ehsan, S. Ahmad, R. Uddin, **T.Rungrotmongkol**, S.S. Azam*, Proteome-wide identification of epitope-based vaccine candidates against multi-drug resistant Proteus mirabilis, *Biologicals* **2018**, 55, 27-37
84. S. Thompho, O. Saengsawang, **T. Rungrotmongkol**, N. Kungwan, S. Hannongbua*, Structure and Electronic Properties of Deformed Single-Walled Carbon Nanotubes: Quantum Calculations, *Structural Chemistry*, **2018**, 29(1): 39-47
85. J. Kicuntod, W. Sangpheak, M. Mueller*, P. Wolschann, H. Viernstein, S. Yanaka, K. Kato, W. Chavasiri, P. Pongsawasdi, N. Kungwan, **T. Rungrotmongkol*** , Physical and biological properties of pinostrobin/β-cyclodextrins inclusion complexes, *Scientia Pharmaceutica*, **2018**, 86(5), 1-15.
86. P. Srivarangkul, W. Yuttithamnon, A. Suroengrit, S. Pankaew, K. Hengprasartporn, **T. Rungrotmongkol**, P. Phuwaphriasirisarn, A. Balasubramanian, R. Padmanabhan, S. Boonyasuppayakorn*, A novel flavanone derivative inhibits dengue virus fusion and infectivity, *Antiviral Research*, **2018**, 151:27-38.
87. Y. Asad, S. Ahmad, **T. Rungrotmongkol**, S.S. Azam*, Immuno-informatics Driven Proteome-wide Investigation Revealed Novel Peptide-based Vaccine Targets Against Emerging Multiple Drug Resistant Providencia stuartii, *Journal of Molecular Graphics and Modeling*, **2018**, 80, 238–250

88. S. Meephon, T. **Rungrotmongkol**, N. Kaiyawet, S. Puttamat, V. Pavarajarn*, Surface-dependence of adsorption and its influence on heterogeneous photocatalytic reaction: A case of photocatalytic degradation of linuron on zinc oxide, *Catalysis Letter*, **2018**, 148: 873-881.
89. S. Ahmad, S. Raza, Qurat-ul-Ain, **T. Rungrotmongkol**, S.S. Azam*, From phylogeny to protein dynamics: A computational hierarchy quest for potent drug identification against an emerging enteropathogen "Yersinia enterocolitica", *Journal of Molecular Liquids*, **2018**, 265: 372-389
90. C. Hanpaibool, T. Chakcharoensap, Arifin, Y. Hijikata, S. Irle, P. Wolschann, N. Kungwan, P. Pongsawasdi, P. Ounjai*, **T. Rungrotmongkol***, Theoretical analysis of orientations and tautomerization of genistein in β-cyclodextrin, *Journal of Molecular Liquids*, **2018**, 265: 16-23.
91. **T. Rungrotmongkol***, T. Chakcharoensap, P. Pongsawasdi, N. Kungwan, P. Wolschann, The inclusion complexation of daidzein with β-cyclodextrin and 2,6-dimethyl-β-cyclodextrin: a theoretical and experimental study, *Monatshefte fur Chemie - Chemical Monthly*, **2018**, 149(10), 1739-1747
92. N. Kongtaworn, N. Hirun, V. Tantishaiyakul, **T. Rungrotmongkol**, S. Dokmaisrijan*, Molecular Aggregation of Four Modified Xyloglucan Models in Aqueous Solution, *Chiang Mai University Journal of Natural Sciences*, **2018**, 45(5), 2201-2210
93. A. Maiuthed, N. Bhummaphan, S. Luanpitpong, A. Mutirangura, C. Aporntewan, A. Meeprasert, **T. Rungrotmongkol**, Y. Rojanasakul, P. Chanvorachote*, Nitric oxide promotes cancer cell dedifferentiation by disrupting an Oct4: caveolin-1 complex: A new regulatory mechanism for cancer stem cell formation, *Journal of Biological Chemistry*, **2018**, 293 (35), 13534-13552, DOI: 10.1074/jbc.RA117.000287
94. N. Jiwalak, R. Daengngern, **T. Rungrotmongkol**, S. Jungsuttiwong, S. Namuangruk, N. Kungwan, S. Dokmaisrijan*, A spectroscopic study of indigo dye in aqueous solution: A combined experimental and TD-DFT study, *Journal of Luminescence*, **2018**, 204, 568-572
95. P. Kanyaboon, T. Saelee, A. Suroengrit, K. Hengphasatporn, **T. Rungrotmongkol**, W. Chavasiri, S. Boonyasuppayakorn*, Cardol triene inhibits dengue infectivity by targeting kl loops and preventing envelope fusion, Scientific Report, **2018**, 8(1):16643
96. J. Phanich, S. Threeracheep, N. Kungwan, **T. Rungrotmongkol***, S. Hannongbua, Glycan binding and specificity of viral influenza neuraminidases by classical molecular dynamics and replica exchange molecular dynamics simulations, *Journal of Biomolecular Structure & Dynamics*, **2019**, 37(13):3354-3365
97. K. Hengphasatporn, N. Kungwan, **T. Rungrotmongkol***, Binding pattern and susceptibility of epigallocatechin gallate against envelope protein homodimer of Zika virus: A molecular dynamics study, Journal of Molecular Liquids, **2019**, 274, 140-147
98. K. Sangpheak, M. Mueller, N. Darai, P. Wolschann*, C. Suwattanasophon, R. Ruga, W. Chavasiri, S. Seetaha, K. Choowongkomon, N. Kungwan, C. Rungnim, **T. Rungrotmongkol***, Computational screening of chalcones acting against topoisomerase IIα and their cytotoxicity towards cancer cell lines, *Journal of Enzyme Inhibition and Medicinal Chemistry*, **2019**, 34(1), 134-143
99. P. Mahalapbutr, K. Thitinanthavet, T. kedkham, N. Huy, T. Le,S. Dokmaisrijan, L. Huynh, N. Kungwan, **T. Rungrotmongkol*** , A theoretical study on the molecular encapsulation of luteolin and

pinocembrin with various derivatized beta-cyclodextrins, Journal of Molecular Structure, **2019**, 1180, 480-490

100.S. Kongkaew, T. **Rungrotmongkol***, C. Punwong, H. Noguchi, F. Takeuchi, N. Kungwan, P. Wolschann, S. Hannongbua*, Interactions of HLA-DR and Topoisomerase I Peptide Modulated Genetic Risk for Diffuse Cutaneous Systemic Sclerosis, Scientific Reports, **2019**, 9, 745

101.H.A.A. Karim, T. **Rungrotmongkol**, S.M. Zain, N.A. Rahman, C. Tayapiwattana, V.S. Lee*, Designed Antiviral Ankyrin – A Computational Approach to Combat HIV-1 via Intracellular Pathway by Targetting the Viral Capsid of HIV-1, Journal of Molecular Liquids, **2019**, 277, 63-69

102.W. Panman, P .Mahalapbutr, O. Saengsawang, C. Rungnim, N. Kungwan, T. Rungrotmongkol*, S. Hannongbua*, Conjugated biopolymer-assisted the binding of polypropylene toward single-walled carbon nanotube: A molecular dynamics simulation, Chiang Mai University Journal of Natural Sciences, **2019**, 46(X): 1-11

103.K. Kerdpol, J. Kicuntod, P. Wolschann, S. Mori, C. Rungnim, M. Kunaseth, H. Okumura, N. Kungwan*, T. Rungrotmongkol*, Cavity Closure of 2-Hydroxypropyl-*β-cyclodextrin*: Replica Exchange Molecular Dynamics Simulations, Polymers, **2019**, 11, 145

104.J. Kammarabut, P. Mahalapbutr, B. Nutho, N. Kungwan, T. Rungrotmongkol*, Lower susceptibility of asunaprevir against R155K and D168A single mutations in HCV NS3/4A protease by molecular dynamics simulation, Journal of Molecular Graphics and Modelling, **2019**, 89, 122-130

105.K. Sangpheak, L. Tabtimmai, S. Seetaha, C. Rungnim, W. Chavasirid, P. Wolschann, K. Choowongkomon, T. Rungrotmongkol*, Biological evaluation and molecular dynamics simulation of chalcone derivatives as EGFR-tyrosine kinase inhibitors, Molecules, **2019**, 24(6), 1092

106.B. Nutho, A.J. Mulholland*, T. Rungrotmongkol*, Quantum Mechanics/Molecular Mechanics (QM/MM) Calculations Support a Concerted Reaction Mechanism for the Zika Virus NS2B/NS3 Serine Protease with Its Substrate, Journal of Physical Chemistry B, **2019**, 123, 13, 2889-2903

107.P. Mahalapbutr, P. Wonganan*, W. Chavasiri, T. Rungrotmongkol*, Butoxy mansonone G inhibits STAT3 and Akt signaling pathways in non-small cell lung cancers: Combined experimental and theoretical investigations, Cancers, **2019**, 11, 437

108.W. Hotarat, C. Rungnim, P. Wolschann, N. Kungwan, T. **Rungrotmongkol***, S. Hannongbua*, Encapsulation of alpha-mangostin and hydrophilic beta-cyclodextrins revealed by all-atom molecular dynamics simulations, Journal of Molecular Liquids, **2019**, 288, 110965

109.S. Meephon, T. **Rungrotmongkol**, S. Puttamat, V. Pavarajarn*, Heterogeneous photocatalytic degradation of diuron on zinc oxide: Influence of surface-dependent adsorption on kinetics, degradation pathway, and toxicity of intermediates, Journal of Environmental Science, **2019**, 84, 97-111

110.S. Ubonprasert, J. Jaroensuk, W. Pornthanakasem, N. Kamonsutthipaijit, P. Wongpituk, P. Mee-udorn, T. Rungrotmongkol, O. Ketchart, P. Chitnumsub, U. Leartsakulpanich, P. Chaiyen, S. Maenpuen*, A flexible flap motif of human cytosolic serine hydroxymethyltransferase is important for quaternary structure stabilization, cofactor and substrate binding, and control of product release, Journal of Biological Chemistry, **2019**, 294(27):10490-10502

111. B. Nutho, A.J. Mulholland*, **T. Rungrotmongkol***, Reaction Mechanism of Zika Virus NS2B/NS3 Serine Protease Inhibition by Dipeptidyl Aldehyde: A QM/MM Study, Physical Chemistry Chemical Physics, **2019**, 21(27), 14945-14956

112. P. Mahalapbutr, N. Darai, W. Panman, A. Opasmahakul, N. Kungwan, S. Hannongbua, T. **Rungrotmongkol***, Atomistic mechanisms underlying the activation of G protein-coupled sweet receptor heterodimer mediated by sugar alcohol recognition:A molecular dynamics study, Scientific Reports, **2019**, 9, 10205

113. C. Yibcharoenporn, P. Chusuth, **T. Rungrotmongkol**, W. Chavasiri, V. Chatsudthipong, C. Muanprasat*, Discovery of a novel chalcone derivative inhibiting CFTR chloride channel via AMPK activation and its anti-diarrheal application, Journal of Pharmacological Sciences, **2019**, 140(3), 273

114. B. Nutho, **T. Rungrotmongkol***, Binding Recognition of Substrates in NS2B/NS3 Serine Protease of Zika virus Revealed by Molecular Dynamics Simulations, Journal of Molecular Graphics and Modelling, **2019**, 2(92), 227-235

115. T. Kaburaki, H. Nakahara, T. Tanaka, K. Okinaga, H. Kawashima, Y. Hamasaki, **T. Rungrotmongkol**, S. Hannongbua, H. Noguchi, M. Aihara, F. Takeuchi, Lymphocyte proliferation induced by high-affinity peptides for HLA-B*51:01 in Behçet's uveitis, PLoS ONE, **2019**, 14(9), e0222384

116. P. Mahalapbutr, P. Wonganan, T. Charoenwongpaiboon, W. Chavasiri, M. Prousoontorn, T. Rungrotmongkol*, Inclusion complexes of mansonone G with β-cyclodextrins: Molecular modeling, phase solubility, characterization, and cytotoxicity. Biomolecules, **2019**, 9(10), 545

117. T. Boonma, B. Nutho, T. Rungrotmongkol, N. Nunthaboot*, Understanding of the drug resistance mechanism of hepatitis C virus NS3/4A to Paritaprevir due to D168N/Y mutations: A molecular dynamics simulation perspective, Computational Biology and Chemistry. **2019**, 83, 107154

118. K. Sanachai, P. Mahalapbutr, K. Choowongkomon, R.P. Poo-arporn, P. Wolschann, T. Rungrotmongkol*, Insights into the binding recognition and susceptibility of tofacitinib toward Janus kinases, ACS Omega, **2019**, 5, 369-377

119. C. Hanpaibool, M. Leelawiwat, K. Takahashi, **T. Rungrotmongkol***, Source of oseltamivir resistance due to single E119D and double E119D/H274Y mutations in pdm09H1N1 influenza neuraminidase, Journal of Computer-Aided Molecular Design, **2020**, 34(1):27-37

120. S. Rattanaphan, **T. Rungrotmongkol**, P. Kongsunea*, Biogas improving by adsorption of CO_2 on modified and unmodified waste tea activated carbon, Renewable Energy, **2020**, 622-631

121. K. Hengphasatporn, A. Garon, P. Wolschann, T. Langer, S. Yasuteru, T.H.N. Thanh, W. Chavasiri, T. Saelee, S. Boonyasuppayakorn, **T. Rungrotmongkol***, Multiple Virtual Screening Strategies for the Optimization of the Novel Compound Against Dengue Virus: A Drug Discovery Study, Sci. Pharm., **2020**, 88, 2

122. A. Sangkaew, N. Samritsakulchai, K. Sanachai, T. Rungrotmongkol, W. Chavasiri, C. Yompakdee*, Novel human carbonic anhydrase isozyme II inhibitors from Murraya paniculata detected by a resazurin yeast-based assay, Journal of Microbiology and Biotechnology, **2020**, 30(4):552-560

123. S. Kitdumrongthum, S. Reabroi, K. Suksen, P. Tuchinda, B. Munyoo, P. Mahalapbutr, **T. Rungrotmongkol**, P. Ounjai, A. Chairoungdua*, Inhibition of topoisomerase IIα and induction of DNA

damage in cholangiocarcinoma cells by altholactone and its halogenated benzoate derivatives, Biomedicine & Pharmacotherapy, **2020**, 127, 110149

124. K. Petsri, M. Yokoya, S. Tungsukruthai, **T. Rungrotmongkol**, B. Nutho, C. Vinayanuwattikun, N. Saito, M. Takehiro, R. Sato, P. Chanvorachote, Structure–Activity Relationships and Molecular Docking Analysis of Mcl-1 Targeting Renieramycin T Analogues in Patient-derived Lung Cancer Cells, Cancers **2020**, *12*(4), 875

125. K. Hengphasatporn, K. Plaimas, A. Suratanee, P. Wongsriphisant, J.-M. Yang, Y. Shigeta, W. Chavasiri, S. Boonyasuppayakorn, **T. Rungrotmongkol***, Target Identification using Homopharma and Network-based Method for Predicting Compounds against Dengue Virus-Infected Cell, Molecules **2020**, *25*(8), 1883

126. J. Kammarabutr, P. Mahalapbutr, H. Okumura, P. Wolschann, **T. Rungrotmongkol***, Structural dynamics and susceptibility of anti-HIV drugs against HBV reverse transcriptase, Journal of Biomolecular Structure and Dynamics **2020**, 20, 10-10

127. B. Nutho[a], P. Mahalapbutr[a], K. Hengphasatporn, N.C. Pattaranggoon, N. Simanon, Y. Shigeta, S. Hannongbua, **T. Rungrotmongkol***, Why Are Lopinavir and Ritonavir Effective against the Newly Emerged Coronavirus 2019? Atomistic Insights into the Inhibitory Mechanisms, Biochemistry, **2020**, 59, 18, 1769–1779

128. E. Lythell, R. Suardiaz, P. Hinchliffe, C. Hanpaibool, S. Visitsatthawong, S. Oliveira, E. Lang, P. Surawatanawong, V.S. Lee, **T. Rungrotmongkol**, N. Fey, J. Spencer*, A.J. Mulholland*, Resistance to the "Last Resort" Antibiotic Colistin: A Single-Zinc Mechanism for Phosphointermediate Formation in MCR Enzymes, Chem. Commun., **2020**, 56, 6874-6877

129. W. Hotarat, B. Nutho, P. Wolschann, **T. Rungrotmongkol***, S. Hannongbua*, Delivery alpha-mangostin using cyclodextrins through a biological membrane: Molecular dynamics simulation, Molecules, **2020**, 25, 2532

130. B. Nutho, S. Pengthaisong, A. Tankrathok, V.S. Lee, J.RK. Cairns*, **T. Rungrotmongkol***, S. Hannongbua*, Structural and Energetic Basis for β-Glucosidase Specificity of Os3BGlu7 by High Structural Similarity of Glucoimidazole and Mannoimidazole Binding, Biomolecules, **2020**, 10(6): 907

131. P. Mahalapbutr, V.S. Lee, **T. Rungrotmongkol***, Binding hot spot and activation mechanism of maltitol and lactitol toward human T1R2-T1R3 sweet taste receptor, Journal of Agricultural and Food Chemistry, **2020**, 68(30), 7974–7983

132. P. Mahalapbutra, M. Sangkhawasib, J. Kammarabutra, S. Chamni*, **T. Rungrotmongkol***, Rosmarinic acid as a potent influenza neuraminidase inhibitor: In vitro and in silico study, Current Topics in Medicinal Chemistry, **2020**, 20, 2046-2055

133. S. Boonyasuppayakorn*, T. Saelee, P. Visitchanakun, A. Leelahavanichkul, K. Hengphasatporn, Y. Shigeta, T.N.T Huynh, J.J.H Chu, **T. Rungrotmongkol**, W. Chavasiri, Dibromopinocembrin and dibromopinostrobin are potential anti-dengue leads with mild animal toxicity, Molecules, **2020**, 25, 4154

134. P. Mahalapbutr, N. Kongtaworn, **T. Rungrotmongkol***, Structural Insight into the Recognition of S-Adenosyl-L-Homocysteine and Sinefungin in SARS-CoV-2 Nsp16/Nsp10 RNA Cap 2'-O-Methyltransferase, Computational and Structural Biotechnology Journal, **2020**, 18, 2766-2773

135. N. Darai, P. Mahalapbutr, K. Sangpheak1, C. Rungnim, P. Wolschann, N. Kungwan, **T. Rungrotmongkol***, In silico screening of chalcones against Epstein-Barr virus nuclear antigen 1 protein, Songklanakarin J. Sci. Technol. **2020**, 42 (4), 802-810

136. H.S.H. Soe, P. Mahalapbutr, N. Kongtaworn, **T Rungrotmongkol**, S. Chamni, P. Jansook*, The investigation of binary and ternary sulfobutylether-β-cyclodextrin inclusion complexes with asiaticoside in solution and in solid state, Carbohydrate Research, **2020**, 498, 108190

137. T. Somboon, P. Mahalapbutr, K. Sanachai, P. Maitarad, V.S. Lee, S. Hannongbua, **T. Rungrotmongkol***, Computational study on peptidomimetic inhibitors against SARS-CoV-2 main protease, Journal of Molecular Liquids, **2021**, 322, 114999

138. Q. Sun, K. Jin, Y. Huang, J. Guo, **T. Rungrotmongkol**, P. Maitarad*, C. Wang*, Influence of conformational change of chain unit on the intrinsic negative thermal expansion of polymers, Chinese Chemical Letters, **2021** DOI: 10.1016/j.cclet.2020.09.046

139. K. Verma, P. Mahalapbutr, A. Auepattanapong, O. Khaikate, C. Kuhakarn, K. Takahashi, **T. Rungrotmongkol***, Molecular Dynamics Simulations on Sulfone Derivatives in Complex with DNA Topoisomerase IIα ATPase Domain, Journal of Biomolecular and Structure Dynamics, **2021** DOI: 10.1080/07391102.2020.1831961

140. J. Jewboonchu, J. Saetang, D. Saeloh, T. Siriyong, **T. Rungrotmongkol**, S.P. Voravuthikunchai, V. Tipmanee*, Atomistic insight and modeled elucidation of conessine towards Pseudomonas aeruginosa efflux pump, Journal of Biomolecular Structure and Dynamics, **2021**, DOI: 10.1080/07391102.2020.1828169

141. T. Roongcharoen, S. Impeng, C. Chitpakdee, **T. Rungrotmongkol**, T. Jitwatanasirikul, S. Jungsuttiwong, S. Namuangruk*, Intrinsic property and catalytic performance of single and double metal atoms incorporated *g-C3N4* for O2 activation: A DFT insight, Applied Surface Science, **2021**, 541, 148671

142. T. Tanawattanasuntorn, T. Thongpanchang, **T. Rungrotmongkol**, C. Hanpaibool, P. Graidist, V. Tipmanee*, (-)-Kusunokinin as a potential aldose reductase inhibitor: Equivalency observed via AKR1B1 dynamics simulation, ACS Omega, **2021**, 6, 1, 606−614

143. P. Murali, K. Verma, **T. Rungrotmongkol**, V.T. Perarasu, K Ramanathan*, Targeting the Autophagy Specific Lipid Kinase VPS34 for Cancer Treatment: An Integrative Repurposing Strategy, The Protein Journal, **2021**, doi.org/10.1007/s10930-020-09955-4 (Quartile score: -, Impact factor 2018: 1.097)

144. T. Boonma, B. Nutho, N. Darai, **T. Rungrotmongkol**, N. Nunthaboot*, Exploring of paritaprevir and glecaprevir resistance due to A156T mutation of HCV NS3/4A protease: Molecular dynamics simulation study, Journal of Biomolecular Structure & Dynamics, **2021** 10.1080/07391102.2020.1869587 (Quartile score: Q2, Impact factor 2018: 2.924)

145. W. Innok, A. Hiranrat, N. Chana, **T. Rungrotmongkol**, P. Kongsune*, In silico and in vitro anti-AChE activity investigations of consituents from Mytragyna speciosa for Alzheimer' s disease treatment, Journal of Computer-Aided Molecular Design, **2021**, doi.org/10.1007/s10822-020-00372-4

146. K. Karnchanapandh, C. Hanpaibool, P. Mahalapbutr, **T. Rungrotmongkol***, Source of oseltamivir resistance due to single E276D, R292K, and double E276D/R292K mutations in H10N4 influenza neuraminidase, Journal of Molecular Liquids, **2021**, 326, 115294

147. K. sangpheak, D. Waraho-Zhmayev, K. Haonoo, S. Torpaiboon, T. Teacharsripaiboon, **T. Rungrotmongkol**, R. Poo-arporn*, Investigation of interactions between binding residues and solubility of grafted humanized anti-VEGF IgG antibodies expressed as full-length format in the cytoplasm of a novel engineered E.coli SHuffle strain, RCS Advances, **2021** accepted

148. N. Bhat, B. Nutho, A. Vangnai, K. Takahashi, **T. Rungrotmongkol***, Substrate binding mechanism of glycerophosphodiesterase towards organophosphate pesticides, Journal of Molecular Liquids, **2021**, 329 115526

149. K. Kerdpol, R. Daengngern, C. Sattayanon, S. Namuangruk, **T. Rungrotmongkol**, P. Wolschann, N. Kungwan*, S. Hannongbua*, Effect of Water Microsolvation on Excited-State Proton Transfer of 3-Hydroxyflavone Enclosed in γ-Cyclodextrin, Molecules, **2021**, 26(4), 843

150. K. Sanachai[a], T. Aiebchun[a], P. Mahalapbutr, S. Seetaha, L. Tabtimmai, P. Maitarad, I. Xenicacis, A. Geronikaki, K. Choowongkomon, **T. Rungrotmongkol***, Discovery of novel JAK2 and EGFR inhibitors from thiazole derivatives, RSC Medicinal Chemistry, **2021** accepted (Prof#5)

151. K. Verman, P. Mahalapbutr, U. Suriya, T. Somboon, T. Aiebchun, L. Shi, P. Maitarad, **T. Rungrotmongkol***, Exploring DNA GyraseB Inhibitors for the Treatment of Clostridium difficile Infection from PhytoHub database using Computational Strategy, Brazilian Archives of Biology and Technology, **2021**, accepted

152. H.E. Putri, B. Nutho, **T. Rungrotmongkol**, B. Sritularak, C., Vinayanuwattikun, P. Chanvorachote, A Bibenzyl Analogue DS-1 Inhibits MDM2-mediated p53 Degradation and Sensitizes Apoptosis in Lung Cancer Cells, Phytomedicine, **2021** accepted

153. T. Aiebchun, P. Mahalapbutr, A. Auepattanapong, O. Khaikate, S. Seetaha, L. Tabtimmai, C. Kuhakarn, K. Choowongkomon*, **T. Rungrotmongkol***, Identification of vinyl sulfone derivatives as EGFR tyrosine kinase inhibitor: In vitro and in silico studies, Molecules, **2021** 26, 2211

154. P. Satapornpong, J. Pratoomwun, P. Rerknimitr, J. Klaewsongkram, N. Nakkam, **T. Rungrotmongkol**, P. Konyoung, N. Saksit, A. Mahakkanukrauh, W. Amornpinyo, U. Khunarkornsiri, T. Tempark, K. Wantavornprasert, P. Jinda, N. Koomdee, T. Jantararoungtong, T. Rerkpattanapipat, C.W. Wang, D. Naisbitt, W. Tassaneeyakul, M. Pirmohamed, W.H. Chung, C. Sukasem, HLA-B*13:01 is a predictive marker of dapsone-induced severe cutaneous adverse reactions in Thai patients, Frontiers in Immunology, **2021**, accepted

155. P. Mahalapbutr, C. Phongern, N. Kongtaworn, S. Hannongbua, T. Rungrotmongkol*, Molecular encapsulation of a key odor-active 2-acetyl-1-pyrroline in aromatic rice with β-cyclodextrin derivatives, Journal of Molecular Liquids, **2021** accepted

โครงการวิจัย	การปรับปรุงสมบัติทางกายภาพของนาโนคอมโพสิตของพอลิโพรพิลีนและท่อนาโนคาร์บอนด้วยการเติมพอลิเมอร์ชีวภาพ: การจำลองพลวัตเชิงโมเลกุล
แหล่งทุน	ทุนวิจัย กองทุนรัชดาภิเษกสมโภช ปีงบประมาณ 2562 (ครั้งที่ 37)
หัวหน้าโครงการ	ศาสตราจารย์ ดร.สุพจน์ หารหนองบัว
ส่วนงาน	ภาควิชาชีวเคมี คณะวิทยาศาสตร์

แบบสรุปผลการวิจัยฉบับสมบูรณ์

.....

รายงานช่วงระยะตั้งแต่วันที่ 1 พฤษภาคม 2562 ถึงวันที่ 30 เมษายน 2563

ชื่อหัวหน้าโครงการ : ศาสตราจารย์ ดร.สุพจน์ หารหนองบัว

หน่วยงาน : ภาควิชาชีวเคมี คณะวิทยาศาสตร์

1. วัตถุประสงค์โครงการ :

1.1 ศึกษาอันตรกิริยาระหว่างพอลิเมอร์ชีวภาพกับสารประกอบเชิงซ้อนระหว่างไอโซแทคติกพอลิโพรพิลีนและท่อนาโนคาร์บอน

1.2 ค้นหาสารตัวเติมพอลิเมอร์ชีวภาพที่สามารถช่วยให้นาโนคอมโพสิตของพอลิโพรพิลีนและท่อนาโน คาร์บอนยึดเกาะกันได้ดีขึ้น

1.3 ศึกษาความสามารถของระบบนำส่งยาด้วยท่อนาโนฮอร์นที่ปรับปรุงด้วยไคโตซานและไซโคลเด็กทรินซ์

2. การดำเนินงาน : [X] ได้ดำเนินงานตามแผนงานที่ได้วางไว้ทุกประการ

[ ] ได้เปลี่ยนแปลงแผนงานที่ได้วางไว้ดังนี้คือ

3. สรุปผลการดำเนินงาน

สรุปผลการดำเนินงานเมื่อเทียบกับแผนที่วางไว้และที่จะดำเนินงานต่อในช่วงเวลาที่เหลือ (ควรระบุผลผลิต/ผลที่คาดว่าจะได้รับให้ชัดเจนและสามารถตรวจสอบและวัดได้ เช่น ผลงานตีพิมพ์ในวารสารวิชาการนานาชาติ/หนังสือ/สิทธิบัตร, ความก้าวหน้าในการสร้างทีมวิจัย, การนำผลจากโครงการไปใช้ประโยชน์ เป็นต้น)

กิจกรรมตามแผนงาน	ผลการดำเนินงาน ครั้งที่ 1	
	ผลผลิตที่ระบุไว้	ผลผลิตที่เกิดขึ้นจริง
โครงการที่ 1 การปรับปรุงสมบัติทางกายภาพของนาโนคอมโพสิตของพอลิโพรพิลีนและท่อนาโนคาร์บอนด้วยการเติมพอลิเมอร์ชีวภาพ: การจำลองพลวัตเชิงโมเลกุล		
1. สร้างแบบจำลองของอะไมโลส ไคโตซาน พอลิโพรพิลีนและท่อนาโนคาร์บอน	ได้โครงสร้างอิสระของอะไมโลส ไคโตซาน พอลิโพรพิลีนและท่อนาโนคาร์บอน	ได้โครงสร้างอิสระของอะไมโลส ไคโตซาน พอลิโพรพิลีนและท่อนาโนคาร์บอน
2. สร้างโครงสร้างเริ่มต้นของสารประกอบเชิงซ้อนระหว่างพอลิโพรพิลีน และท่อนาโน คาร์บอนที่พันรอบด้วยอะไมโลส และไคโตซาน	ได้โครงสร้างเริ่มต้นที่ใช้ในการคำนวณขั้นต่อไป	ได้โครงสร้างเริ่มต้นที่ใช้ในการคำนวณขั้นต่อไป
3. จำลองพลวัตเชิงโมเลกุลที่อุณหภูมิ 298 K เป็นเวลา 200 นาโนวินาที	ได้โครงสร้างที่เก็บได้ จากการคำนวณโดยวิธีการจำลองพลวัติเชิงโมเลกุลเป็นเวลา 200 นาโนวินาที	ได้โครงสร้างที่เก็บได้ จากการคำนวณโดยวิธีการจำลองพลวัติเชิงโมเลกุลเป็นเวลา 200 นาโนวินาที
4.วิเคราะห์ชนิดของอันตรกิริยาและสมบัติเชิงโครงสร้าง ระหว่างพอลิเมอร์ชีวภาพกับท่อนาโนคาร์บอน/พอลิโพรพิลีน	ได้ข้อมูลพื้นฐานเชิงโมเลกุลที่สำคัญความเข้าใจถึงพฤติกรรมและยึดจับกันระหว่างพอลิเมอร์ชีวภาพและท่อนาโนคาร์บอน/พอลิโพรพิลีน	ได้ข้อมูลพื้นฐานเชิงโมเลกุลที่สำคัญความเข้าใจถึงพฤติกรรมและยึดจับกันระหว่างพอลิเมอร์ชีวภาพและท่อนาโนคาร์บอน/พอลิโพรพิลีน
5. วิเคราะห์ สรุปผล และเขียนผลงานเพื่อตีพิมพ์ในวารสารระดับนานาชาติ	ได้ผลงานตีพิมพ์ในวารสารระดับนานาชาติจำนวน 1 เรื่อง	ได้ผลงานตีพิมพ์ในวารสารระดับนานาชาติจำนวน 1 เรื่อง
โครงการที่ 2 ระบบนำส่งยาต้านมะเร็งด้วยท่อนาโนฮอร์นที่ปรับปรุงด้วยไคโตซานและไซโคลเด็กทรินซ์: การจำลองพลวัตเชิงโมเลกุล		
1. สร้างพารามิเตอร์ของท่อนาโนฮอร์น ไซโคลเด็กทรินซ์ ไคโตซาน และยาด็อกโซรูบิซินด้วยวิธีการคำนวณเชิงควอนตัม		ได้พารามิเตอร์ที่จำเป็นในการจำลองพลวัติเชิงโมเลกุล
2. สร้างโครงสร้างเริ่มต้นของสารประกอบเชิงซ้อนระหว่าง (i) ท่อนาโนฮอร์นกับยา (ii) ท่อนาโนฮอร์นพันด้วยไคโตซานกับยา (iii) ท่อนาโนฮอร์นพันด้วยไคโตซานและไซโคลเด็กทรินซ์กับยา		ได้โครงสร้างเริ่มต้นของระบบนำส่งยา 3 รูปแบบ
3. จำลองพลวัตเชิงโมเลกุลที่อุณหภูมิ 298 K เป็นเวลา 500 นาโนวินาที		

4.วิเคราะห์ชนิดของอันตรกิริยา สมบัติเชิงโครงสร้าง และกลไกการขนส่งยาด็อกโซรูบิซินจากระบบนำส่งยาแบบต่างๆ 5. วิเคราะห์ข้อมูลเปรียบเทียบกับผลการทดลอง สรุปผล และเขียนผลงานเพื่อตีพิมพ์ในวารสารระดับนานาชาติ		ได้โครงสร้างที่เก็บได้ จากการคำนวณโดยวิธีการจำลองพลวัติเชิงโมเลกุลเป็นเวลา 500 นาโนวินาที ได้ข้อมูลพื้นฐานเชิงโมเลกุลที่สำคัญความเข้าใจถึงพฤติกรรมและยึดจับกันระหว่างยากับท่อนาโนฮอร์น ยากับไคโตซานที่พันรอบท่อนาโนฮอร์น และยากับไซโคลเด็กทรินซ์ที่ต่อกับไคโตซานที่พันรอบท่อนาโนฮอร์น ได้บทความวิจัยเพื่อตีพิมพ์เผยแพร่ในวารสารระดับนานาชาติจำนวน 1 เรื่อง

4. การดำเนินงานในช่วงต่อไป

-

5. กิจกรรมอื่นๆ ที่เกี่ยวข้อง (ได้แก่ การไปเสนอผลงาน, การได้รับเชิญเป็นวิทยากร, การได้รับรางวัล, การเชื่อมโยงทางวิชาการกับนักวิชาการอื่นๆ ทั้งในประเทศและต่างประเทศ เป็นต้น)

5.1 การได้รับรางวัล

-

5.2 การได้รับเชิญเป็นวิทยากร และการนำเสนอผลงานในงานประชุม

-

5.3 การได้รับเชิญเป็นวิทยากรสัมมนา

-

6. อุปสรรคในการดำเนินงาน และแนวทางแก้ไข

เนื่องจากการระบาดของโรคติดเชื้อไวรัสโคโรนา 2019 จึงได้เพิ่มขอบเขตการวิจัยในการศึกษาความสามารถของระบบนำส่งยาต้านมะเร็งด้วยท่อนาโนฮอร์นที่ปรับปรุงด้วยไคโตซานและไซโคลเด็กทรินซ์ด้วยวิธีทางเคมีคอมพิวเตอร์ โดยใช้งบประมาณจากหมวดค่าใช้จ่ายการเชิญผู้เชียวชาญต่างประเทศ และค่า Cloud computing

7. ความเห็นของผู้วิจัย (กรณีมีการเปลี่ยนแปลงในปัจจัยภายนอกโครงการอย่างไร เช่น กฎเกณฑ์ นโยบาย ความร่วมมือกับหน่วยงาน ฯลฯ)

-

8. เอกสารแนบ (ถ้ามี เช่น reprint หรือ manuscript / ข้อมูล จากโครงการ / บทคัดย่อ หรือบทสรุปของบทความวิชาการ หรือเอกสารในลักษณะอื่นๆ ตลอดจนสื่อประเภทต่างๆ ที่โครงการได้จัดทำขึ้น / ผลงานอื่นๆ ที่เกี่ยวข้อง)
ผลงานตีพิมพ์ในวารสารระดับนานาชาติจำนวน 1 เรื่อง และอยู่ในระหว่างดำเนินเตรียมบทความเพื่อส่งตีพิมพ์ 1 เรื่อง

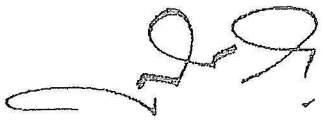

.....

ศาสตราจารย์ ดร.สุพจน์ หารหนองบัว

(หัวหน้าโครงการวิจัย)

...../...../.....

Chiang Mai J. Sci. 2019; 46(3) : 547-557
http://epg.science.cmu.ac.th/ejournal/
Contributed Paper

Conjugated Biopolymer-assisted the Binding of Polypropylene Toward Single-walled Carbon Nanotube: A Molecular Dynamics Simulation

Wanwisa Panman [a], Panupong Mahalapbutr [b], Oraphan Saengsawang [c], Chompoonut Rungnim [d], Nawee Kungwan [e,f], Thanyada Rungrotmongkol*[b,g] and Supot Hannongbua*[h]

[a] Multidisciplinary Program of Petrochemistry and Polymer Science, Faculty of Science, Chulalongkorn University, Bangkok 10330, Thailand.
[b] Structural and Computational Biology Research Unit, Department of Biochemistry, Faculty of Science, Chulalongkorn University, 254 Phayathai Road, Bangkok 10330, Thailand.
[c] Office of Corporate R&D, IRPC Public Company Limited, Rayong, 21000, Thailand.
[d] National Nanotechnology Center (NANOTEC), National Science and Technology Development Agency (NSTDA), Pathum Thani 12120, Thailand.
[e] Department of Chemistry, Faculty of Science, Chiang Mai University, Chiang Mai 50200, Thailand
[f] Research Center on Chemistry for Development of Health Promoting Products from Northern Resources, Faculty of Science, Chiang Mai University, Chiang Mai 50200, Thailand.
[g] Ph.D. Program in Bioinformatics and Computational Biology, Faculty of Science, Chulalongkorn University, Bangkok 10330, Thailand.
[h] Center of Excellence in Computational Chemistry (CECC), Department of Chemistry, Faculty of Science, Chulalongkorn University, Bangkok 10330, Thailand.

*Author for correspondence; e-mail: thanyada.r@chula.ac.th; supot.h@chula.ac.th

Received: 9 October 2018
Revised: 5 December 2018
Accepted: 6 December 2018

ABSTRACT

Nowadays the nanocomposite materials have shown to be the key applications in a wide range of industries due to their unique properties such as thermal and electrical properties. Polymer/carbon nanotube (CNT) nanocomposite is one of interesting nanocomposite materials manufactured for improving mechanical, thermal and electrical properties of polymer. Unfortunately, polypropylene (PP)/CNT preparation is difficult because of CNT dispersion and aggregation. In this study, amylose (AMY) and chitosan (CS) are selected in order to study how biopolymer could diminish such problems by non-covalent modification on outer surface of single-walled CNT using molecular dynamics (MD) simulations. The results reveal that AMY can induce the atactic, isotactic and syndiotactic PPs contacting with CNT exterior surface in spiral-shape, while these PPs are aligned in snake-shape by CS modification instead. Additionally, electrostatic force is the main interaction for a complexation of CNT/biopolymer/PPs.

Keywords : nanocomposite materials, carbon nanotube, amylose, polypropylenes, molecular dynamics simulation

1. INTRODUCTION

Nanocomposite is a multiphase solid material in which at least one of the phases shows dimensions of less than 100 nanometers called "nanofillers" or "nanoparticles" [1]. The addition of nanofillers in ceramic, metal and polymer can enhance the thermal and mechanical properties, including toughness as well as electrical and thermal conductivities. The examples of nanofillers added to composite are clay, gold particle and carbon nanotube [2-3]. Applications of nanocomposites can be used as capacitors, car components and in drug delivery [4-5].

Carbon nanotubes (CNTs) are members of the fullerene structural family discovered by "Sumio Ijima" in 1991 [6]. CNTs are tube-shaped materials with diameter in nanometer scale and length up to several centimeters. They have high curvature and extra-large surface area. CNTs are composed of one carbon atom linked to three other carbon atoms by covalent bonds [7]. CNTs are attractive to research interests due to their unique properties such as high electrical and thermal conductivities, excellent stiffness against bending, high tensile strength, highly flexible, low mass density, very elastic and good electron field emitters [8]. They are made up from folding of graphene sheet, in which one sheet of graphene produces single-walled carbon nanotube (SWCNT) with diameter of around 0.4 nanometer, while the folding of multiple sheets becomes multi-walled carbon nanotube (MWCNT) with diameter of around 100 nanometers [2-3].

Polymer/CNT nanocomposites comprise a polymer or copolymer with CNT nanofiller. CNT is used as nanofiller in polymer for improving the mechanical, thermal and electrical properties of polymer [9-12]. In this work, the polypropylene (PP)/CNT nanocomposite is focused. PP is widely used in many industries due to its several beneficial properties, including low mass, high tensile strength and chemical resistance. However, it shows the low properties of thermal stability as well as electrical conductivity [13-14]. Thus, the addition of CNT into polymer matrix is able to improve those properties. Deng and co-worker [15] investigated the dispersion of CNT in PP/CNT nanocomposite using scanning electron microscopy (SEM) and they found that CNTs were aggregated and showed a poor dispersion in polymer matrix, leading to a difficulty in synthesis of PP/CNT nanocomposite. Moreover, Syamol and co-worker [10] indicated that isotactic polypropylene (iPP) could poorly wrap around CNT outer surface and the intramolecular interactions within iPP units were also found using molecular dynamics (MD) simulation.

A biopolymer with notable chemical and biological properties is amylose (AMY). It is biocompatibility, biodegradability, and nontoxicity [16]. AMY is formed by α-D-glucose units through α(1→4) glycosidic bonds [17]. Zang and co-worker [18] added AMY and the other polysacccarides into CNTs for investigation of cell behavior. They found that AMY, which can wrap around CNT, led to a decrease in the CNT aggregation and to enhance cell adhesion. In addition, Xie and co-worker [19] studied the intermolecular interactions between AMY and CNT using MD simulations at 300 K. The results showed that AMY wrapped around CNT outer surface through van der Waals interaction and it could encapsulate into CNT cavity. Basu and co-worker [20] investigated the blending of AMY/PP. They suggested that AMY can interact with PP, leading to an enhancement of melt flow index of PP. Chitosan (CS) is a well-known functional material due to its excellent properties such as biocompatibility, non-toxicity and adsorption properties [21]. By investigation of cell behavior, Zang and co-worker [18] found that CS, which can wrap around the outer surface of CNT, decreased the aggregation of CNT and increased cell

adhesion. Aztatzi-Pluma and co-worker [22] used MD simulation for studying interactions between different degrees of deacetylation (DD) of chitosan and CNT at 300 K for 3.5 ns. The MD results displayed that chitosan at 60% of DD showed the strongest interaction with CNT. Salmah and co-workers [23] revealed that adding CS and modified CS into PP matrix could help to increase the young modulus and thermal properties.

Although, the previous studies suggested that these two biopolymers can interact with PPs or CNT, the formulation of CNT/biopolymer/PPs has not yet known. Therefore, in the present work, we aimed to theoretically elucidate the effect of AMY or CS non-covalently modified on SWCNT towards the binding of the three different PPs (atactic polypropylene (aPP), isotactic polypropylene (iPP) and syndiotactic polypropylene (sPP)) using molecular dynamics simulation. Moreover, the intermolecular interactions of PPs with CNT and modified CNTs are compared.

2. MATERIALS AND METHODS

2.1 Molecular Models of Amylose, Polypropylene and Carbon Nanotube

The 3D structures of AMY containing 30 units of alpha-D-glucose and the two models of 60%DD chitosan (CS) containing 30 (30CS) and 50 units (50CS) were constructed using the tLEaP module implemented in AMBER 16. The three types of polypropylene (PP), including atactic polypropylene (aPP), isotactic polypropylene (iPP) and syndiotactic polypropylene (sPP) consisting of 30 repeating units of PP were generated using the Material Studio 5.5 Suite [21]. Note that, the methyl groups are randomly positioned in aPP form, whereas the methyl groups are constructed along the same side and alternate side of the polymer chain in iPP and sPP systems, respectively. The (10,0) zigzag of single-walled CNT with a diameter of 7.8 Å, chiral vectors n = 10 and m = 0, containing 30 repeating units was built using the Material Studio 5.5 Suite. Subsequently, the CNT was wrapped spirally with each biopolymer in according to the previous research [18-19]. Each PP was placed in parallel with the length (x axis) of CNT. AMY and CS were parameterized by Glycam_06j-1 force field [25], while PPs and CNT were treated by the General Amber Force Field (GAFF). In total, there are twelve generated systems without and with AMY or CS as shown in Figure 1.

2.2 Molecular Dynamics (MD) Simulation

MD simulation was performed under vacuum condition using AMBER16 package with the NVT ensemble at 1 atm and 298 K using a time step of 2 fs. The SHAKE algorithm [26] was applied to all bonds involving hydrogen atoms. The long-range electrostatic interactions were calculated using the Particle Mesh Ewald (PME) summation method. All systems were heated up to 298 K for 100 ps and equilibrated at 298 K for 5 ns. Finally, the production stage was performed until 100 ns and the structural coordinates were saved every 2 ps for analysis. The root mean square displacement (RMSD), radius of gyration (Rg) and van der Waals and Electrostatic interactions were calculated by the cpptraj module implemented in AMBER16, while the distance between the centers of gravity of each polymer unit and CNT was computed with FORTRAN script [6].

3. RESULTS AND DISCUSSION

3.1 System Stability

To estimate the system stability of the CNT/PPs nanocomposites without and with biopolymer non-covalent modification on the external surface of SWCNT, the RMSD of each system relative to the minimized structure was calculated along the simulation time and plotted in Figure 2. The RMSD values of all three PPs (dark green) on CNT rapidly increase at the first 60 ns and fluctuate in the range of

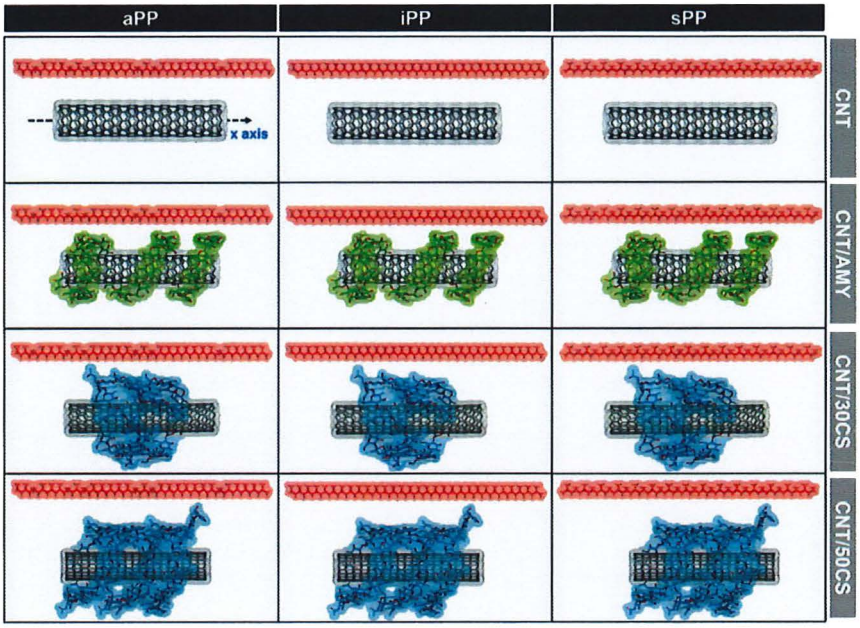

Figure 1. The initial models of CNT/PPs nanocomposite without and with AMY (green), 30CS and 50CS (blue) modification for MD study: PP (red) was placed in parallel with the X axis of CNT and biopolymer was spirally wrapped around CNT surface.

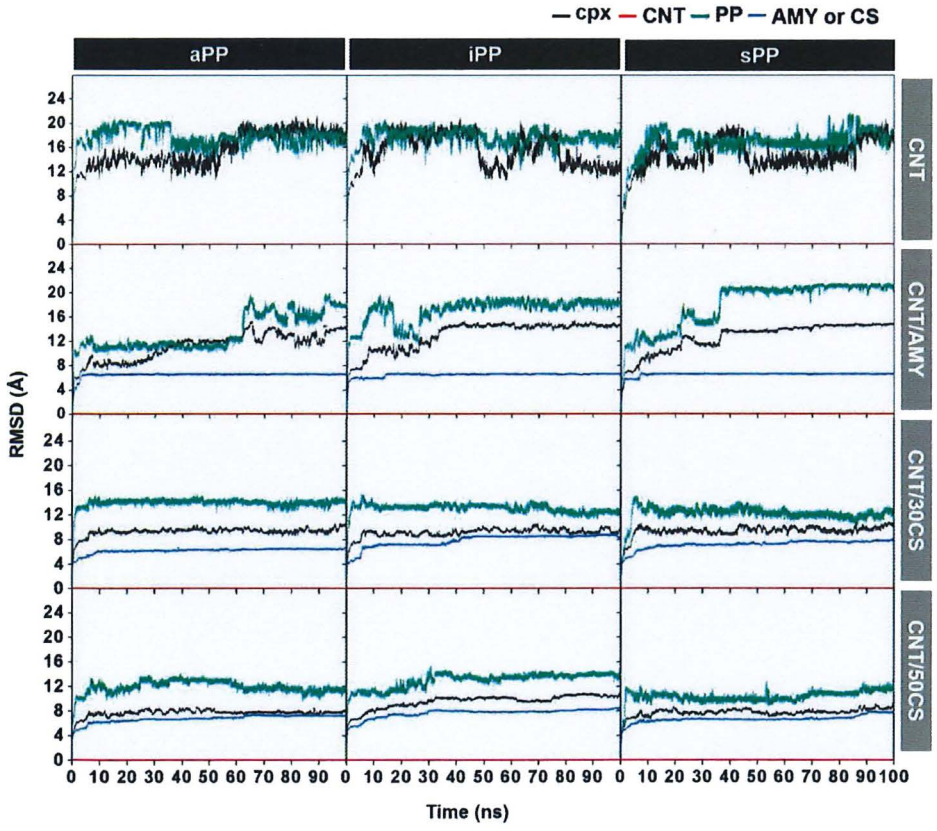

Figure 2. All-atoms RMSDs of complex (black), CNT (red), PP (dark green) and biopolymer (blue) relative to their minimized structures for all systems of CNT/PPs nanocomposite without and with biopolymer modification on tube surface.

~16-20 Å until the end of the simulations. In case of AMY wrapped on CNT, the RMSD values of PP show relatively lower fluctuation and reached the equilibrium state after ~40 ns for the CNT/AMY/iPP and CNT/AMY/sPP systems and after ~60 ns for the CNT/AMY/aPP system. This is in contrast to AMY, in which the RMSD of 6 Å compared to its initial structure with a very low fluctuation is observed along the simulations in these three systems. For CS modified systems, the RMSD values of PP and CS (blue) enhance at the first 10 ns and then maintain at ~11-12 Å and ~4-6 Å, respectively. As expected, no structural change of CNT is detected as evidenced by RMSD close to 0 Å. Taken together, this is therefore the atomic coordinates of each system in the last 40 ns were collected for further analysis.

Polypropylene binding toward carbon nanotube

The final orientation of PPs and AMY or CS on CNT outer surface taken from the last MD snapshot of each system was depicted in Figure 3. In case of pristine CNT, the results reveal that all three PPs preferentially interact within themselves on CNT surface and do not spirally wrap around the tube, in a strong correlation with previous studies [12, 27]. Interestingly, the biopolymer conjugating on CNT could enhance the efficacy of PPs bindings to become significantly locate closer toward CNT with a formation of a spiral- or snake-shaped structure of PPs in case of AMY or CS modification, respectively. However, the steric effect of CS's functional groups is higher than AMY, leading to the lower wrapping efficiency than AMY as evidenced by the distance analysis demonstrating that the d(PP_{Cg} - $CNT_{Surface}$) of AMY is significantly lower than that of CS (Figure 4, discussed later).

In order to compare the direct binding capacity between PPs toward CNT without and with biopolymer conjugation on the external surface, the distances measured from the center of gravity (Cg) of each unit of PPs to surface of CNT (d(PP_{Cg} -$CNT_{Surface}$)) averaged over the last 40 ns were calculated in relative to the distance measured from Cg of each biopolymer unit to surface of CNT (d(AMY_{Cg} - $CNT_{Surface}$) or d(CS_{Cg} - $CNT_{Surface}$)). These distances versus unit of polymer are given in Figure 4. It can be clearly seen that all AMY units well interact with the CNT outer surface with the averaged d(AMY_{Cg} - $CNT_{Surface}$) of ~4 Å (Figure 4b). The AMY wrapping importantly decreases the averaged d(PP_{Cg} - $CNT_{Surface}$) for the iPP and sPP systems from ~8 Å to ~4 Å for the systems without and with AMY non-covalently modification. This finding suggests that CNT/AMY could help these two PPs directly interacts with the CNT outer surface. However, only the 10 aPP units of one end exhibit a similar tight binding on the CNT/AMY, whilst the rest units show a high fluctuation as detected in the previous work [28]. In case of CS modified CNT systems (Figure 4c-d), almost all CS units are in range of 4 to 6 Å according to the CNT/CS/doxorubicin study of 4.4 Å [6]. All PPs favorably interact with both 30CS (d(PP_{Cg}-$CNT_{Surface}$) of 5-10 Å) and 50CS (d(PP_{Cg}-$CNT_{Surface}$) of 6-11 Å) in a snake-like shape rather than show a direct interaction with CNT surface (Figure 3).

Taken together, the use of conjugated biopolymer on CNT exterior leads to an enhanced interfacial adhesion of PPs toward CNT, which is in good agreement with the electrostatic and van der Waals attractions as discussed later.

3.2 Polypropylene Folding

The effect of conjugated biopolymer on polypropylene folding towards CNT is characterized in terms of Rg and end to end distance of PPs. The Rg calculation was used to identify the mean squared distance of each point on the polymer from its center of gravity

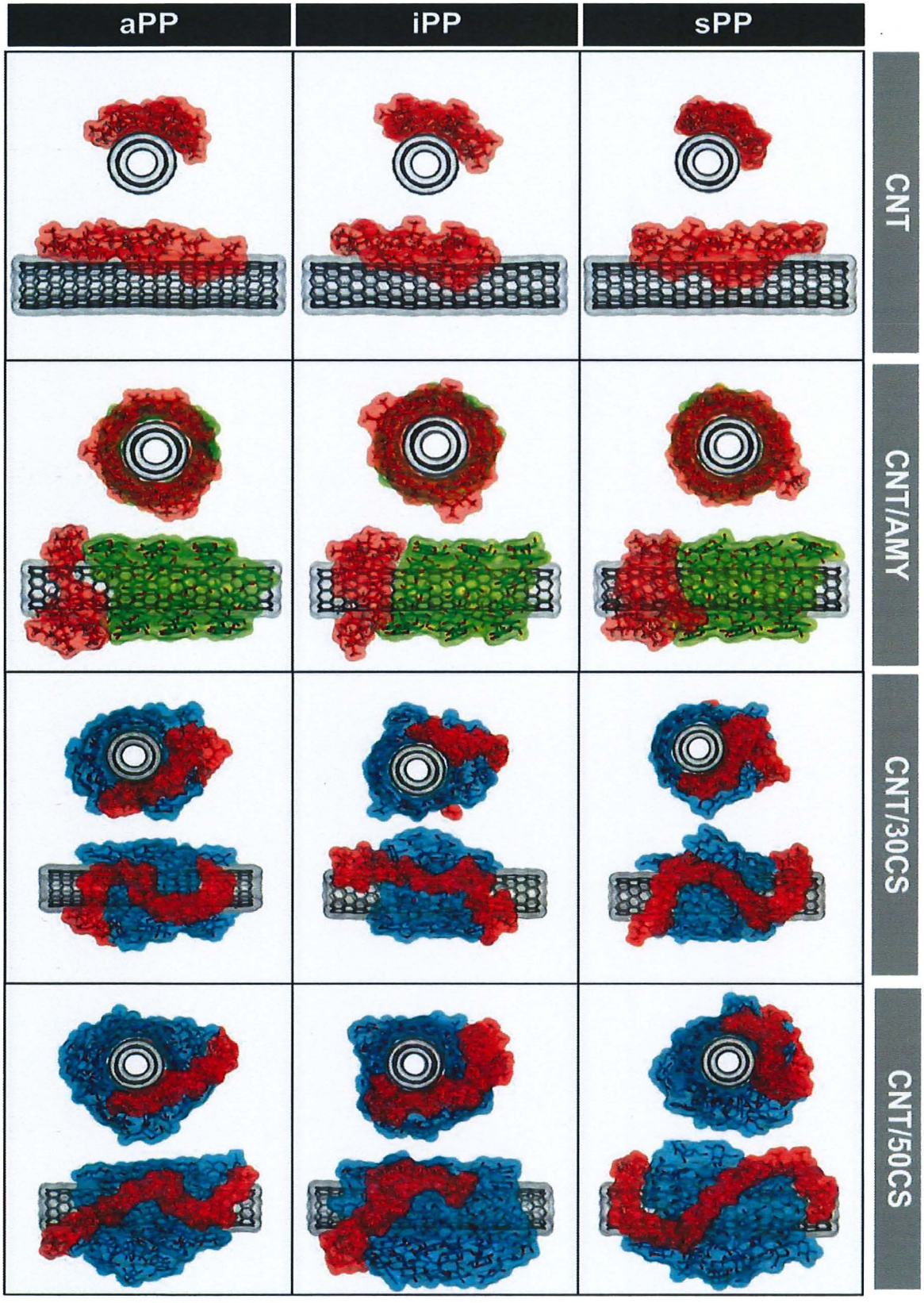

Figure 3. The last MD snapshots of all 12 systems, where PP, AMY, CS, CNT structures are shaded by red, green, blue and gray, respectively.

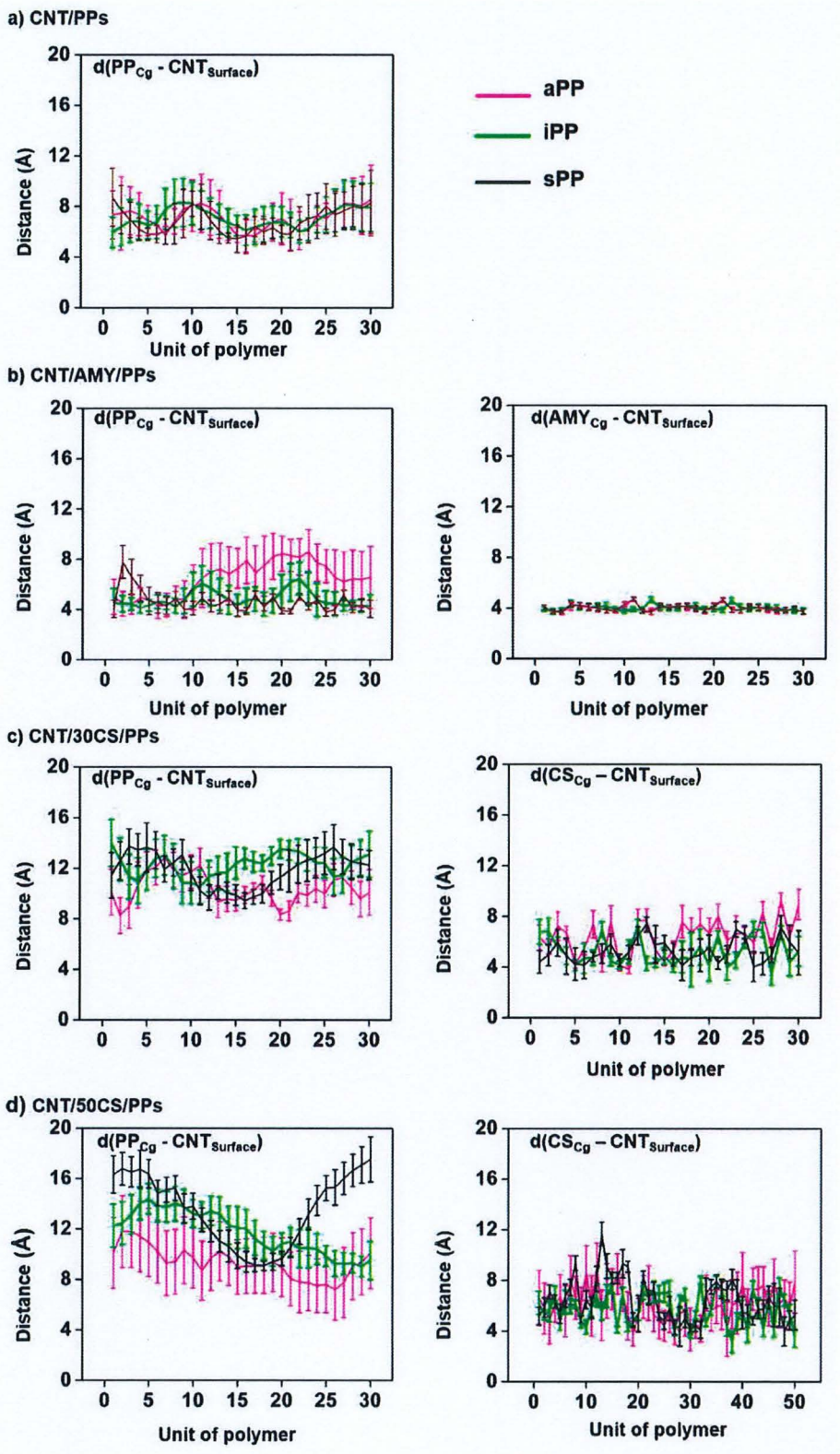

Figure 4. Plots of (left) the averaged distance measured from Cg of each PP unit to CNT surface ($d(PP_{Cg} - CNT_{Surface})$) and (right) the averaged distance measured from Cg of each biopolymer unit to Cg of CNT surface ($d(AMY/CS_{Cg} - CNT_{Surface})$), and $d(PP_{Cg} - CNT_{Surface})$ for the studied systems: a) CNT/PPs, b) CNT/AMY/PPs, c) CNT/30CS/PPs and d) CNT/50CS/PPs.

[29] using equation 1:

$$Rg = \sqrt{\frac{1}{N}\sum_{N}^{i=0}(r_i - r_m)^2} \quad (1)$$

where N is the number of atoms, r_i denotes atomic position and r_m denotes the mean position of all atoms.

As shown in Figure 5, in case of no conjugated biopolymer on CNT, the Rg of all three PPs dramatically reduces within the first 20 ns and consequently retains at the fluctuation of ~8-11 Å until the end of simulation. This is because PPs preferentially interact with each other rather than spirally contact with CNT as described above (see also Figure 3). Interestingly, the use of AMY non-covalently modified on CNT significantly increases the Rg stability of iPP and sPP after 40 ns, reflecting the stable conformation of partial spiral form for these PPs. However, in the aPP system, the Rg fluctuation is similar to that of no AMY conjugation due to the high flexibility of one terminal end, which was also reported previously [30] The reduction of Rg values for all PPs is even faster in CS modified systems (within 5 ns) and fluctuates at ~11 Å until the end of

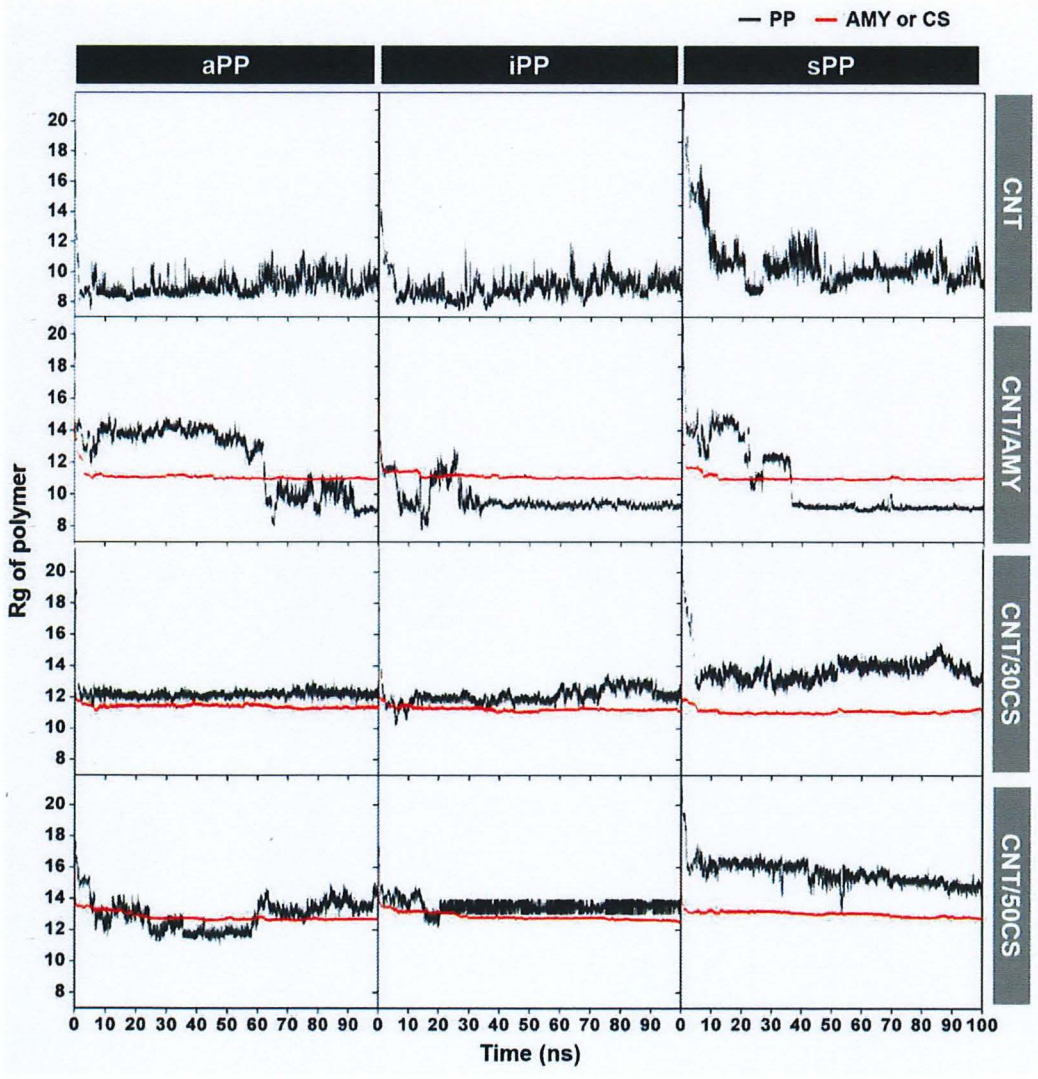

Figure 5. Plots of Rg of polymers, PP (black) and biopolymer AMY or CS (red), versus simulation time for all systems. Distance of end-to-end chain of polypropylene.

simulation. Note that, the Rg plots of either AMY or CS are likely comparable, which is significantly lower than those of PPs in terms of fluctuation as expected.

The distance of end-to-end chain of PPs measured between centers of gravity of the first and last units of PP along simulation period for all systems is plotted in Figure 6. Note that the initial distance of end-to-end chain of PPs is ~70 Å. After 100-ns simulation, such distance is importantly shortening to ~10 Å in iPP and sPP and ~20 Å in aPP for CNT/AMY systems, whilst in almost all CNT/CS systems with two different lengths of CS chain the distance is of ~30 Å. The obtained results can confirm the spiral-shape and snake-like shape of PP folding in CNT/AMY and CNT/CS, respectively (see also Figure 3).

3.3 Electrostatic and Van Der Waals Interactions

The electrostatic (ΔE_{ele}) and van der Waals (ΔE_{vdW}) interaction energies between PP and CNT (or modified CNT) versus simulation time are given in Figure 7. Considering all systems without any modification, the ΔE_{ele} and ΔE_{vdW} values between PPs and CNT are ~2200 kcal/mol and ~ -350 kcal/mol, respectively, suggesting that vdW interaction is the main force for molecular complexation. In case of the systems with AMY non-covalently conjugated on CNT, both interaction energies of all PPs are dramatically reduced to ~ -1500 and ~ - 800 kcal/mol for ΔE_{ele} and ΔE_{vdW}, respectively. Similarly, for all systems with CS wrapping, the ΔE_{ele} and ΔE_{vdW} values are ~ -1000 kcal/mol

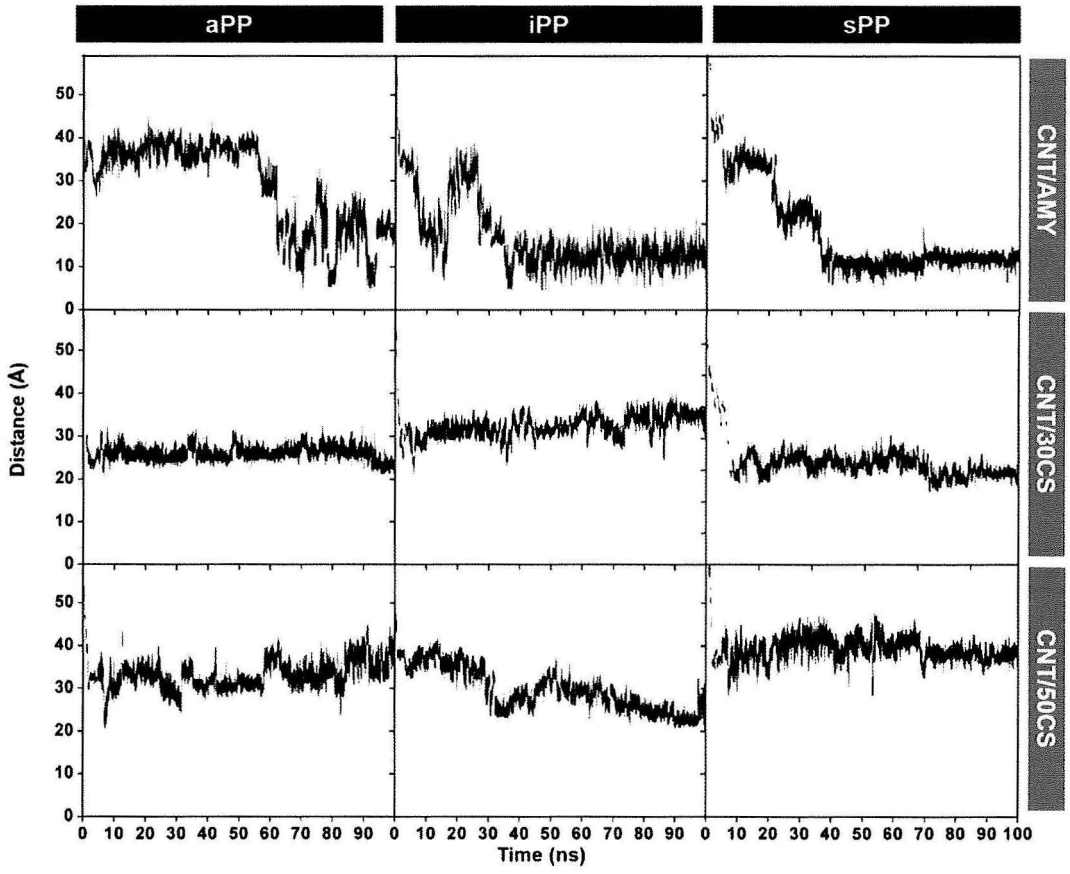

Figure 6. The distance plot of end-to-end chain of PPs versus simulation time for the CNT systems modified by two biopolymers, AMY and CS.

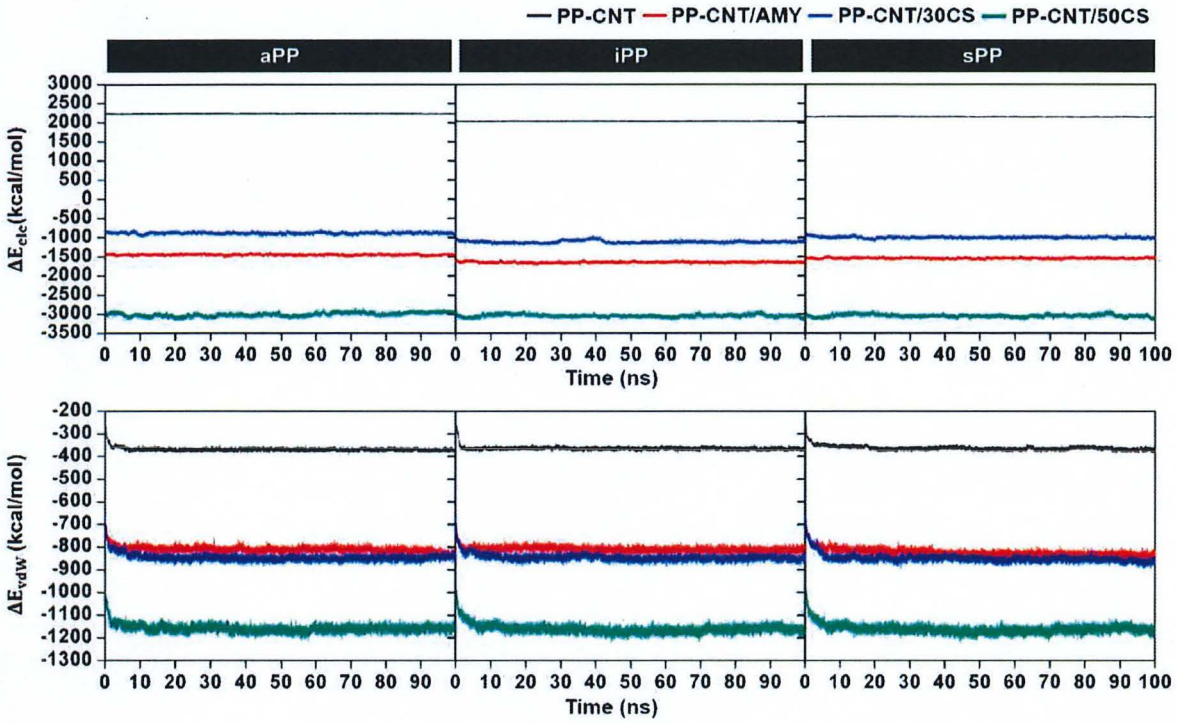

Figure 7. ΔE_{ele} (top) and ΔE_{vdW} (below) of PP with CNT (black), CNT/AMY (red), CNT/30CS (blue) and CNT/50CS (green).

and ~ -800 kcal/mol for CNT/30CS systems and ~ -3000 and ~ -1200 kcal/mol for CNT/50CS systems. From this finding, it can be concluded that two focused biopolymers could promote the binding efficacy of PPs toward CNT through both electrostatic and vdW interactions in accordance with the previous works [11, 19, 44, 46, 48]. By considering the energy difference between the systems without and with non-covalent surface modification, electrostatic attraction is likely found to be the main driving force for CNT/biopolymer/PPs formation.

4. Conclusion

In the present study, the all-atom MD simulations for 100-ns reveal that either AMY or CS non-covalently modified on CNT outer surface could induce the PPs binding toward CNT with a formation of better-formed nanocomposite. While PPs recognize to bind with both AMY and CNT by folding in the spiral-shape around tube surface, the presence of CS introduces the PPs to orientate in the snake-like shape and only interact with CS spirally wrapped around the tube. Moreover, the main interaction causing PPs to become better contact with CNT/biopolymer is electrostatic attraction. Taken together, besides the non-covalent surface modification is able to prevent the CNTs aggregation as well-known, the biopolymer AMY or CS could significantly increase the interfacial adhesion of PPs toward CNT.

Acknowledgements

This work was financially supported by the Ratchadaphiseksomphot Endowment Fund, Chulalongkorn University (CU-GR_62_11_23_05). W.P. thanks the Research and Researchers for Industries (MSD59I0066), the 90th Anniversary of CU Fund (Ratchadaphiseksomphot Endowment fund), and the Overseas Research Experience Scholarship for Graduate Student.

P.M. thanks Science Achievement Scholarship of Thailand. This research work was partially supported by Chiang Mai University. The Center of Excellence in Computational Chemistry (CECC) was acknowledged for facilities and computing resources.

REFERENCES

[1] Mezzenga R. and Ruokolainen J., *Nature Mater.*, 2009; **8**: 926.

[2] Choudhary V. and Gupta A., *Polymer/Carbon Nanotube Nanocomposites*, 4th Edn., InTech, London, 2011

[3] Liu Y. and Kumar S., *ACS Appl. Mater. Interf.*, 2014; **6**: 6069-6087.

[4] Rungrotmongkol T., Arsawang U., Iamsamai C., Vongachariya A., Dubas S.T., Ruktanonchai U., Soottitantawat A. and Hannongbua S., *Chem. Phys. Lett.*, 2011; **507**: 134-137.

[5] Rungnim C., Rungrotmongkol T. and Poo-arporn R. P., *J. Mol. Graph. Model.*, 2016; **70**: 70-76.

[6] Iijima S., *Nature*, 1991; **354**: 56.

[7] Tjong S.C., *Mater. Sci. Eng.*, 2006; **53**: 73-197.

[8] Endo M., Strano M.S. and Ajayan P.M., Potential Applications of Carbon Nanotubes, in Jorio A., Dresselhaus G. and Dresselhaus M.S., eds., *Carbon Nanotubes: Advanced Topics in the Synthesis, Structure, Properties and Applications*, Springer -Verlag Berlin Heidelberg, Heidelberg, 2008: 3-62.

[9] Papageorgiou G.Z., Nerantzaki M., Grigoriadou I., Papageorgiou D.G., Chrissafis K. and Bikiaris D., *Macromol. Chem. Phys.*, 2013: **214(21)**; 2415-2431.

[10] Tallury S.S. and Pasquinelli M.A., *J. Phys. Chem. B*, 2010; **114**: 4122-4129.

[11] Fujigaya T. and Nakashima N., *Sci. Technol. Adv. Mater.*, 2015; **16**: 024802. doi:10.1088/1468-6996/16/2/024802.

[12] Beyer G., *Plastics Additives and Compounding*, 2002; **4**: p. 22-28.

[13] Zhang S. and Horrocks A.R., *Prog. Polym. Sci.*, 2003; **28**: 1517-1538.

[14] Liang J.Z. and. Li R.K.Y., *J. Appl. Polym. Sci.*, 2000; **77**: 409-417.

[15] Deng H., Bilotti E., Zhang R. and Peijis T., *J. Appl. Polym. Sci.*, 2010; **118**: 30-41.

[16] Cai X., Yang L., Zhang L. M. and Wu Q., *Carbohydr. Res.*, 2010; **345(7)**: 922-928.

[17] van der Maarel M.J.E.C., van der Veen B., Uitdehaag J.C.M., Leemhuis H. and Dijkhuizen L., *J. Biotechnol.*, 2002; **94(2)**: 137-155.

[18] Zhang X., Meng L. and Lu Q., *ACS Nano*, 2009; **3**: 3200-3206.

[19] Xie Y.H. and Soh A.K., *Mater. Lett.*, 2005; **59**: 971-975.

[20] Basu D., Datta C. and Banerjee A., *J. Appl. Polym. Sci.*, 2002; **85**: 1434-1442.

[21] Majeti N.V. and Kumar R., *React. Funct. Polym.*, 2000; **46**: 1-27.

[22] Aztatzi-Pluma D., Castrejón-González E.O., Almendarez-Camarillo A., Alvarado J. F. J. and Durán-Morales Y., *J. Phys. Chem. C*, 2016; **120(4)**: 2371-2378.

[23] Salmah H., Amri F. and Kamarudin H., *Polym. Plast. Technol. Eng.*, 2012; **51**: 86-91.

[24] Accelrys Inc, Materials Studio 5.5, 2010.

[25] Kirschner K.N., Yongye A B., Tshampel M.S., GonzaLez-Outeirino J., Daniels C.R., Foley B. L. and Woods R.J., *J. Comput. Chem.*, 2008; **29(4)**: 622-655.

[26] Ryckaert J.P., Ciccotti G. and Berendsen H.J.C., *J. Comput. Phys.*, 1977; **23**; 327-341.

[27] Yang S., Yu S. and Cho M., *Carbon*, 2013; **55**: 133-143.

[28] Yang J., Lin Y., Wang J., Lai M., Li J., Liu J., Tong X. and Cheng H. , *J. Appl. Polym. Sci.*, 2005; **98(3)**: 1087-1091.

[29] Liu W, Yang C.L., Zhu Y.T. and Wang M.S., *J. Phys. Chem. C*, 2008; **112(6)**: 1803-1811.

[30] Grosberg A.Y., Khalatur P.G. and Khokhlov A.R., *Rapid Commun.*, 1982; **3**: 709-713.

The Use of Pristine and Chitosan Functionalized Carbon Nanohorn as Drug Carrier for Targeted Drug Delivery System in Cancer Therapy

Napat Kongtaworn[1], Bodee Nutho[2], Panupong Mahalapbutr[3], Nutpanai Ustagitavee[3], Chompoonut Rungnim[4], Supot Hannongbua[5] and Thanyada Rungrotmongkol[1,2*]

[1]Program in Bioinformatics and Computational Biology, Graduate School, Chulalongkorn University, Bangkok 10330, Thailand

[2]Center of Excellence in Computational Chemistry (CECC), Department of Chemistry, Faculty of Science, Chulalongkorn University, Bangkok 10330, Thailand

[3]Structural and Computational Biology Research Unit, Department of Biochemistry, Faculty of Science, Chulalongkorn University, Bangkok 10330, Thailand

[4]National Nanotechnology Center (NANOTEC), National Science and Technology Development Agency (NSTDA), Pathum Thani 12120, Thailand

[5]Center of Excellence in Computational Chemistry (CECC), Department of Chemistry, Faculty of Science, Chulalongkorn University, Bangkok 10330, Thailand; supot.h@chula.ac.th

[*]Corresponding authors. TR Fax: +66 2 218-5418; Tel: +66 2 218-5426

E-mail address: thanyada.r@chula.ac.th, chompoonut.run@nectec.or.th

Abstract

Carbon nanohorns (CNHs) are considered as promising drug carriers for cancer therapy. However, the pristine CNHs exhibit low solubility and dispersion in aqueous solution, and especially are high toxicity to our body. To solve such problems, the mixture of biocompatible polymers such as chitosan (CS) and β-cyclodextrin (βCD) with CNHs is rather promising. In this study, we modeled an effective delivery system of doxorubicin anticancer drug in complex with pristine CNH and functionalized CNH. To investigate the loading of anticancer drug, doxorubicin, we prepared an effective drug delivery system for delivery the drug, such as pristine carbon nanohorn system (CNH/DOX), chitosan functionalized CNH system (CS-f-CNH/DOX) and 2,6-dimethyl-β-cyclodextrin (DMBCD) on CS functionalized carbon nanohorn system (CS-f-CNH/DOX/CD). All atom molecular dynamics (MD) simulations were firstly carried out on all types of drug delivery system and then the binding free energy were performed by MMPBSA method. The binding of DOX inside and outside indicated that the binding between DOX and CNH is higher than that between DOX and CS. Moreover, the movement of drug inside and outside CNH surfaces suggest that DOXs can stably move around middle and edge of CNH while the DOXs on CS slightly move around initial CS residues. In conclusion, all data showed that the designed drug delivery systems of CNH and functionalized CNH can be served as drug carrier.

Keywords: Doxorubicin, Carbon nanohorns, chitosan and MD simulation

Introduction

Most people have been concerned about diseases causing death, especially cancers that are considered as the number fifth deadliest diseases in the world in 2018 [1]. In Thailand, female population with breast cancers have dramatically increased every year [2]. Doxorubicin (DOX; Adriamycin) is a potential anticancer drug that is used to treat several types of cancers [3]. It is absorbed into the human body and serves as an intercalating agent between DNA strand, leading to inhibit gene expression and synthesis of biomolecules involved in progression of cancer [3]. This enzyme can release the helicity of supercoil structure of DNA during transcription and regulate topoisomerase II complex after separating of the DNA in DNA replication. When chromaromatic rings of this drug interact with minor grooves of the DNA, they prevent the forming of DNA double helix. In previous study [4], protonated DOXs are used in simulation for investigating drug loading and releasing of carbon nanotube. The main reason why the drug had to be protonated because this simulation will run in pH 7.0.

In fact, anticancer drugs not only target the cancer cells, but also kill the normal cells with the same function. This is the main reason why most patients who are treated with chemotherapy could present many adverse effects [5]. For avoiding the unwanted effects, the anticancer drug will be loaded with targeted drug delivery systems (DDSs) to specific site of action [6]. There were a number of studies that focused on the development of the DDSs, including the use of liposome [7-8], necrosome [9-10], nanoemulsions [11-12], cyclodextrin inclusion complexes [13-14], lipid nanocapsules [15-16], polymeric micelles [17-18], and carbon nanomaterials [19-20]. Ideally, the best suitable systems must have good interactions with drugs and release them at the targeted places [21]. To date, nanomaterials have become one of the great choices for practical uses in DDSs, especially carbon nanomaterials. Specifically, carbon nanohorns (CNHs) have been

attention in recent years. With their lower toxicity, CNHs are more interesting to study as comparison to classical carbon nanotube [22]. Nevertheless, the hydrophobic surface of CNHs usually forms the petal-dahlia-like, dahlia-like, bud-like and seed-like SWNHS aggregates, which is first available for research in experiment way [23].

In the DDSs, there are other kinds of drug carriers, particularly cyclodextrins (CDs) [24]. CDs are naturally divided into three classes depending on the size of the inner cavity that consisted of 6 to 8 glucoses for alpha-, beta- and gamma-CDs, respectively, and connected each glucose subunit with α-1,4 glycosidic linkages [25]. The hydrophobic cavity of CDs forms as turn-acted cone-shape, while the outer surface is relatively hydrophilic. In this study, we decided to choose the beta-type cyclodextrin (or BCD) and their derivatives, such as DMBCD since DMBCD, which functions as a carrier of drugs, has an inner cavity that suits DOX [26-28]. the BCD can conjugate them with chitosan, which improves the system of carrying a greater number of drugs. The conjugated systems are supposed to be the powerful systems for carrying more drugs killing cancer cells at the targeted places [26-28]. Moreover, the DOX is carrier inside and outside pristine CNH and functionalized CNH are simulated using molecular dynamics (MD) simulations and binding free energy were performed by MMPBSA technique to understand the molecular interactions and the movement of DOX within and without CNH and CS functionalized CNH. We hope that this research can help to understand the movement and behavior of DOX with pristine CNH and CS functionalized CNH which have potential as drug carrier.

2. Computational Methods

2.1 Preparation of DOX, CNH, CS and βCD

The geometry of DOX structure was optimized by the HF/6-31(d) level of theory using Gaussian09 program [29]. Moreover, CNH was built by the Material studio program and calculated using Gaussian 09 program at the same level of theory there were parameterized using the General Amber Force Field (GAFF). Furthermore, each molecular sugar of the 60% of degree deacetylation chitosan (CS) chain and β-cyclodextrin (BCD) were generated and parameterized by GLYCAM06 force field. CS chain was constructed from randomly 65 units of 2 different sugars: D-glucosamine (GCS or G) and N-acetyl-D-glucosamine (NAG or N) while BCD ring are constituted by 7 units of α-D-glucopyranoside. In addition, the complexation of DOX and BCD were predicted using molecular docking technique.

The DOX was docked into the cavity of cyclodextrin and calculated interaction energy using Autodock vina program [29]. The poses with the first and second lowest interaction energies of clearly different conformations of DOX (as A-form and B-form in Fig. m1) were selected form 100 different conformations of that as the initial structure for applying to BCD at the first repeating unit of CS chain. DOX in CNH, CS and BCD

2.2 Molecular design of drug delivery systems

The DOX drug and single-walled CNH configurations were prepared as 16 systems in total defined as system 1.1(T), 1.1(M), 1.1(E), 1.2(M), 2.1(T), 2.1(M), 2.1(E), 2.2(M), 3.1(T, A), 3.1(M, A), 3.1(E, A), 3.1(T, B), 3.1(M, B), 3.1(E, B), 3.2(M, A) and 3.2(M, B) (figure 1). The letters T, M and E are abbreviation of tip, middle and edge, respectively. For the system 1.1(M) and 1.2(M), both systems were consisted of one molecule of CNH and DOX. However, there was difference

in positions of DOX molecule inside CNH cavity for system 1.1(M) and outside CNH cavity for system 1.2(M). In system 2.1(M) and 2.2(M), they were additionally wrapped by one chain of CS. Note that the sequence of CS was presented in fig. 1. The 65 units of CS chain were built from the two components: G and N (what are G and N? Please clarify). Each CS unit was bonded together via beta-1.4 linkage in 3:2 ratio of G:N (60% of degree deacetylation) in the simple random sequences of D-glucosamine (GCS or G) and N-acetyl-d-glucosamine (NAG or N) as "GGNGNGNGNNGNGNGNGNNNNGNGNGNGNNGNGNGNGNNNGGNNNGNGNNNGN GNGNGNNNGNGG". The helix-like chitosan was wrapped on the external surface of CNH. Moreover, the CS chain in system 2.1(M) and 2.2(M) were modified by different two DOX-BCD complexes (A-form and B-form) at the first repeating unit of CS chain (system 3.1(M, A) – 3.2(M, B)). In addition to getting suitable regions of DOX within CNH, DOX structures of system 1.1(M), 2.1(M) and 3.1(M) were started at different position of CNH hole such as tip (system 1,1(T), 2,1(T), 3.1(T, A) and 3.1(T, B)), middle (system 1,1(M), 2,1(M), 3.1(M, A) and 3.1(M, B)) and edge (system 1,1(E) 2,1(E), 3.1(E, A) and 3.1(E, B)) of CNH. Then, each system was neutralized with a chlorine ion and solvated with TIP3P water solvent parameter in octagonal box over 15 Å from the complex. MD simulation of all explicit systems were conducted. In this work, parameters for each system was prepared as the same way for MD simulation method [30].

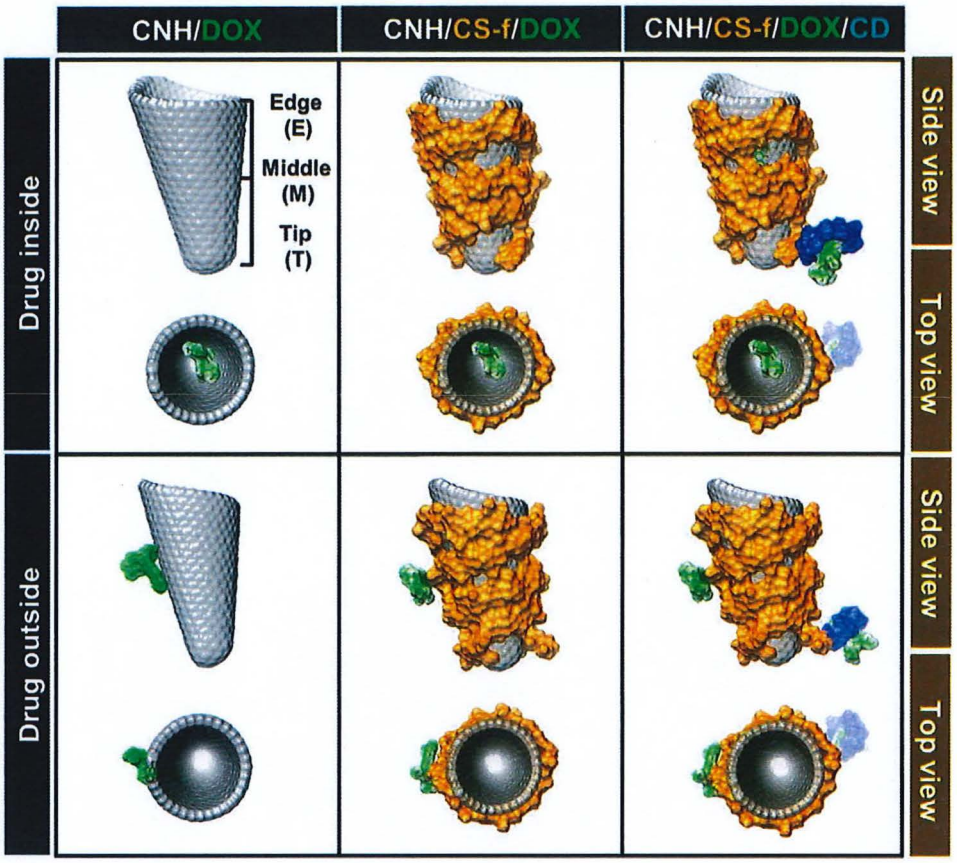

Figure 1. The three-dimension (3D) structures of 14 systems. The CNH (dim grey), CS or CD-f-CS (orange) were presented by their surface while DOXs (C atom in green) are highlighted in stick. E is DOX at edge CNH, M is DOX at middle CNH and DOX is tip CNH.

2.3 Molecular dynamics (MD) simulations

The MD simulation of each system was performed using pmemd.cuda module in AMBER16 package with NVT ensemble at 1 atm and the time of step of 2 fs. The SHAKE algorithm was applied to all bonding hydrogen atoms and cut off function was set at 12 Å for non-boned interaction [31]. The long-range electrostatic interactions were calculated by the Particle Mesh Ewald (PME) summation method [32]. Each system was heated up from 0 K to 300 K for

500 ps and equilibrated at the 300 K for 1 ns with NPT ensemble. Finally, the production state was performed at 300 K until reaching 500 ns. The trajectories of the systems were collected every 2 ps for analysis using CPPTRAJ module in AMBER program and the binding free energy were calculated using The Molecular Mechanics Poisson-Boltzmann Surface Area (MMPBSA) method.

2.4 Binding free energy calculations

The MMPBSA method was used to compute binding free energies of both systems using 1000 snapshots taken from MD trajectories in the last 10 ns. The MMPBSA function to calculate the inhibitor-protein free energy was written as following [33]:

$\Delta G_{bind} = G_{complex} - G_{protein} - G_{ligand}$

$G_{complex}$, $G_{protein}$ and G_{ligand} are the free energy of complex, protein and ligand, respectively. In addition, each the free energy was calculated from the molecular mechanic (E_{MM}), the solvation free energies (G_{solv}) and the entropic contribution (TS). The equations were written as following:

$G = E_{MM} + G_{solv} - TS$

$E_{MM} = E_{bond} + E_{angle} + E_{dihedral} + E_{ele} + E_{vdW}$

$Gsolv = G_{PB} + G_{SA}$

E_{MM} is consist of bonded term as bond angle and dihedral energies (E_{bond}, E_{angle} and $E_{dihedral}$) and non-bonded term as Van der Waals and electrostatic energies (E_{ele} and E_{vdW}). Moreover, G_{solv} was calculated from Poisson–Boltzmann equation (G_{PB}) and the nonpolar contribution (G_{SA}) between the solute and the solvent continuously.

3. Results and Discussion

3.1 Stability and DOX movement of complexes

The distance between center of mass of CNH and DOX were investigated along the simulation time and depicted in Figure 2. For all CNH/DOX_{inside} systems, the DOX molecule initialized placed at the middle of CHN moved out to the edge of CHN with the distance of 0-3 Å for the first 200 ns of simulation. Then, the DOX translocated within a range from 0 to 15 Å till the end of simulation. Likewise, the distance analysis revealed that the DOX molecule, which was placed at the tip of CNH can move to the middle region at the beginning of simulation (~10 ns).

and then translocate within a range of -5 to 15 Å. Instead, the DOX molecule started at the edge of CNH intermediately pointed toward the middle part of CNH in the first 10 ns and slightly fluctuated ~5-10 Å above the center of CNH after 200 ns of simulation. In addition, the distance plot of CS-f-CNH/DOX system, in which the DOX molecule was positioned at the center of CNH can translocate up and down in the range of -10 to 10 Å until reaching 500 ns. The result suggested that the DOX at different 3 initial position of CNH within and without surface of CNH have the same pattern of movement. The DOX can carrier around middle and edge of CNH surface.

For the DOX within CS-f-CNH/DOX and CS-f-CNH/DOX/CD, the movement of DOXs are similar to results of CNH/DOX. However, the movement of DOX on CS and CS/CD chains are different. The DOX move and fluctuate around initial residue of CS all of simulation. The results indicated that DOX on CS chains can interact with CS and CS/CD chains while CS chain wrapped around CNH surface. The stability of DOX movement within and without CNH surface are same pattern. The DOX fluctuate at middle and edge of CNH. Interestingly, the DOX inside CS-f-CNH/DOX/CD present the same pattern of drug movement. The small drug as cisplatin on CNH was investigated [34]. They reported that CNH have ability as drug carrier. the cisplatin fluctuates within the tip of CNH [34] whereas DOX cannot fluctuate around tip of CNH. this is case of steric hindrance of DOX structure.

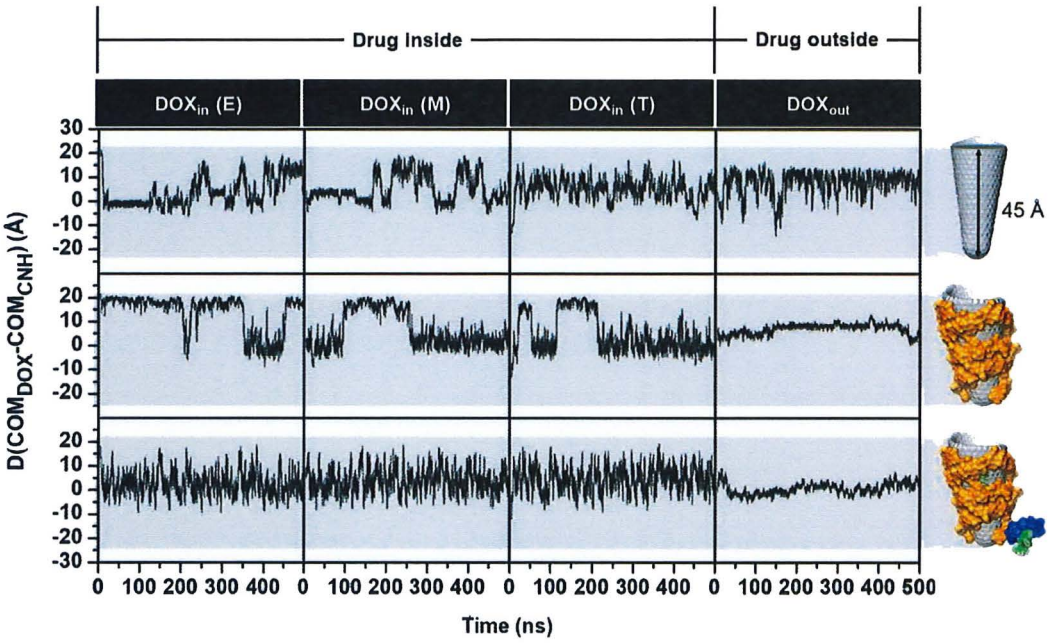

Figure 2. The distance between the center of mass of DOX and CNH.

Apart from the movement of DOX in each system mentioned above, the plots of the distance of DOX and center of mass of CNH versus the distance of DOX and surface of CNH extracted from the last 250 ns are given in Fig. 3. For the systems with DOX located inside the CNH, the distance between center of mass of DOX and CNH surface (Y-axis) showed the similar pattern. The distance was distributed at about 3 Å, while the systems with DOX located outside the CNH showed the high deviation of the distance ranging from 3 to 8.5 Å. This reflected that the DOX molecule can move on the surface of CNH and chitosan. The results of drug outside are different in CS-f-CNH/DOX result. The distance of CS-f-CNH/DOX is about 8 Å. While, the CS-f-CNH/DOX/CD are presented the difference from CS-f-CNH/DOX. The DOX of CS-f-CNH/DOX/CD system move from CS chain to CNH surface that result will represent in contact result.

For the distance between center of DOX and center of CNH (X-axis), the distances of different initial location of DOX within and without CNH were found around -10 to 20 Å. These observations supported that results of drug movement. The DOX fluctuated at the middle and edge of CNH. In addition, the distance between center of DOX and surface DOX are about 3 Å for all results of drug inside. So, the middle initial location of DOX for all drug insides will select to represent the results for others part.

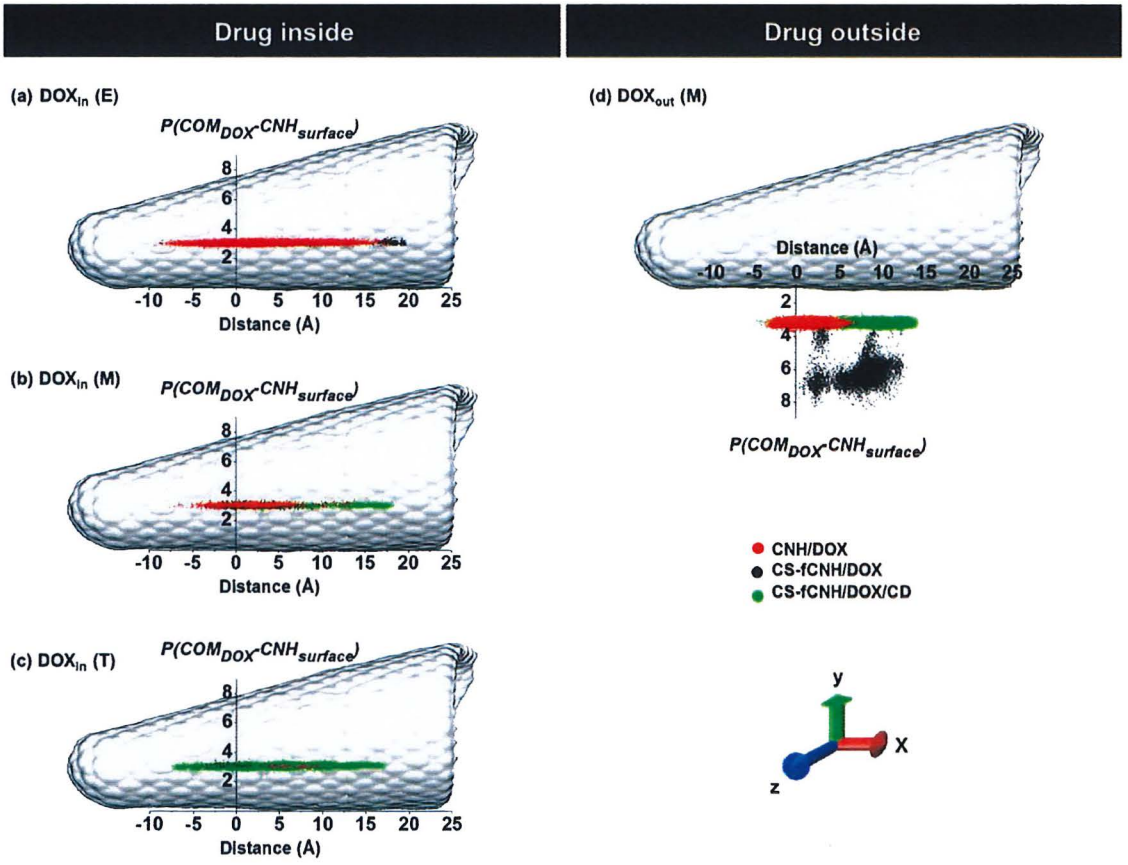

Figure 3. The plot of distance between center of DOX and center of CNH (X-axis) *versus* the distance between center of DOX and CNH surface (Y-axis) for **a**) DOX at the edge of CNH, **b**) DOX at the middle of CNH, **c**) DOX at the tip of CNH and **d**) DOX at the outside of CNH.

The representative last MD snapshots of DOX at the middle of CNH (located inside and outside of CNH) were illustrated in Figure 4. Each DOX from drug inside systems showed the similar conformation to each other. The aromatic ring of DOX was parallel to the surface of CNH, while the sugar moiety of DOX was vertical to the surface of CNH. These results were also similar to the CNH/$DOX_{outside}$ system. The DOX molecule can move along the surface of CNH with the same conformation as observed in the DOX inside system. However, for the CS-f-CNH/$DOX_{outside}$/CD system, there was the large gap of CD-CS chain wrapped on the CNH surface, resulting in the accessible movement of DOX in this gap. For another DOX outside CS-f-CNH, The DOX can move on a chitosan chain. The aromatic ring showed parallel conformation on surface of chitosan while the sugar ring upward from chitosan chain. In addition, the chitosan can wrap around the CNH surface (a snack-like structure). The DOX(A) inside cyclodextrin ring can bind together and the cyclodextrin ring.

In addition to chitosan wrapped on the CNH surface, the average distance between each chitosan residue and CNH surface were showed in Figure 5. Each system displayed the similar trend of the average distance values. The average distance of each residue was found at ~3 to 6 Å. The results indicated that the chitosan can constantly wrap on the outer surface of CNH. However, the CS-f-CNH/$DOX_{outside}$ system showed the distinct value for the first residue. This is because this residue is freely movable without CD bound.

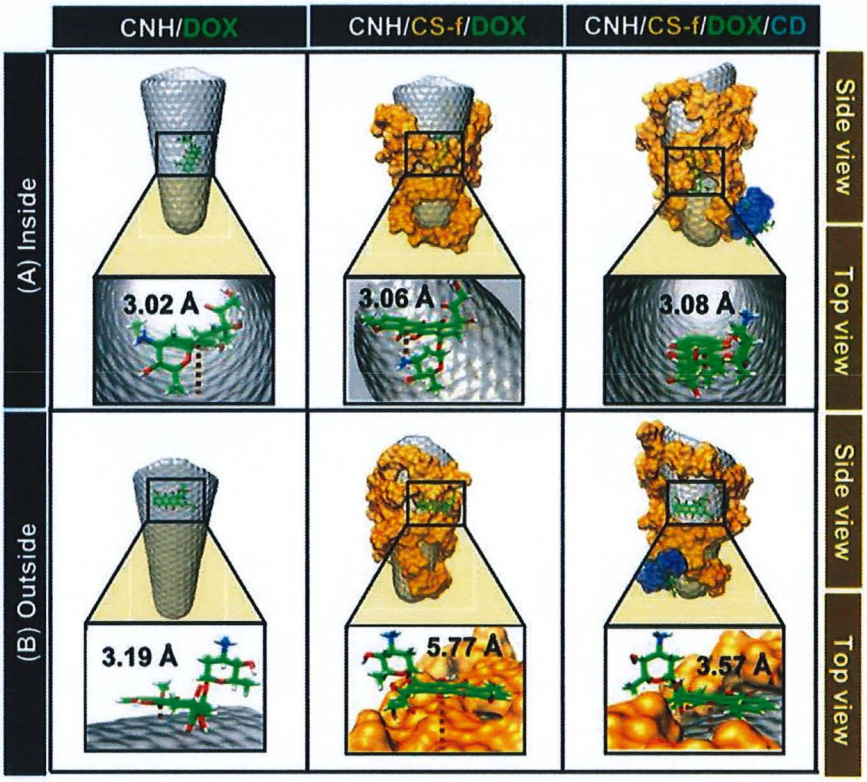

Figure 4. Structure of all DOX at middle of CNH systems and DOX outside systems at 500 ns of dynamics.

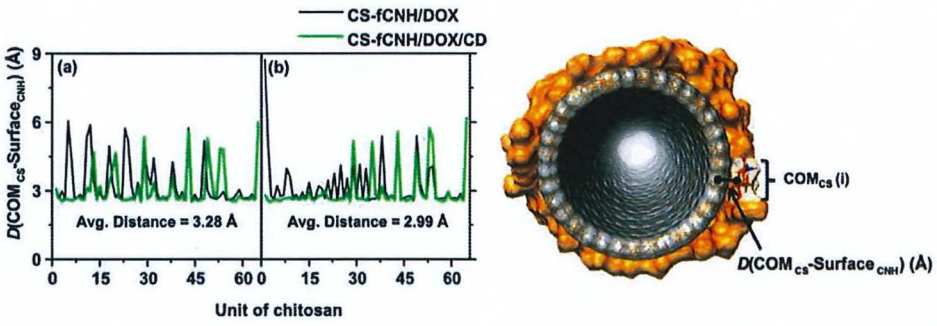

Figure 5. The average distance between chitosan and surface of CNH. left graphs are avg. distance between CNH and chitosan per units (DOX_{inside} systems) and graphs plots are avg. distance between CNH and chitosan per units ($DOX_{outside}$ systems)

3.2 solubility of complex

The water accessibility of each system is calculated by the radial distribution function (RDF), as shown in fig. 7. These plots presented the distribution of water oxygen atom around heteroatoms of DOX. The first solvation shell was found ~3 Å. For DOX_{inside} system, a minimum of the O6, O7, O8, O11 and N atoms shows a movable solvation while other presents a disappearing of the peak in the first solvation shell. For CD-CS-f-CNH system, O10 shows no water was detected within a distance around 3 Å. Moreover, the $DOX_{outside}$ system shows similar results with DOX inside system. However, water accessibility of $DOX_{outside}$ are decreased by CD-CS.

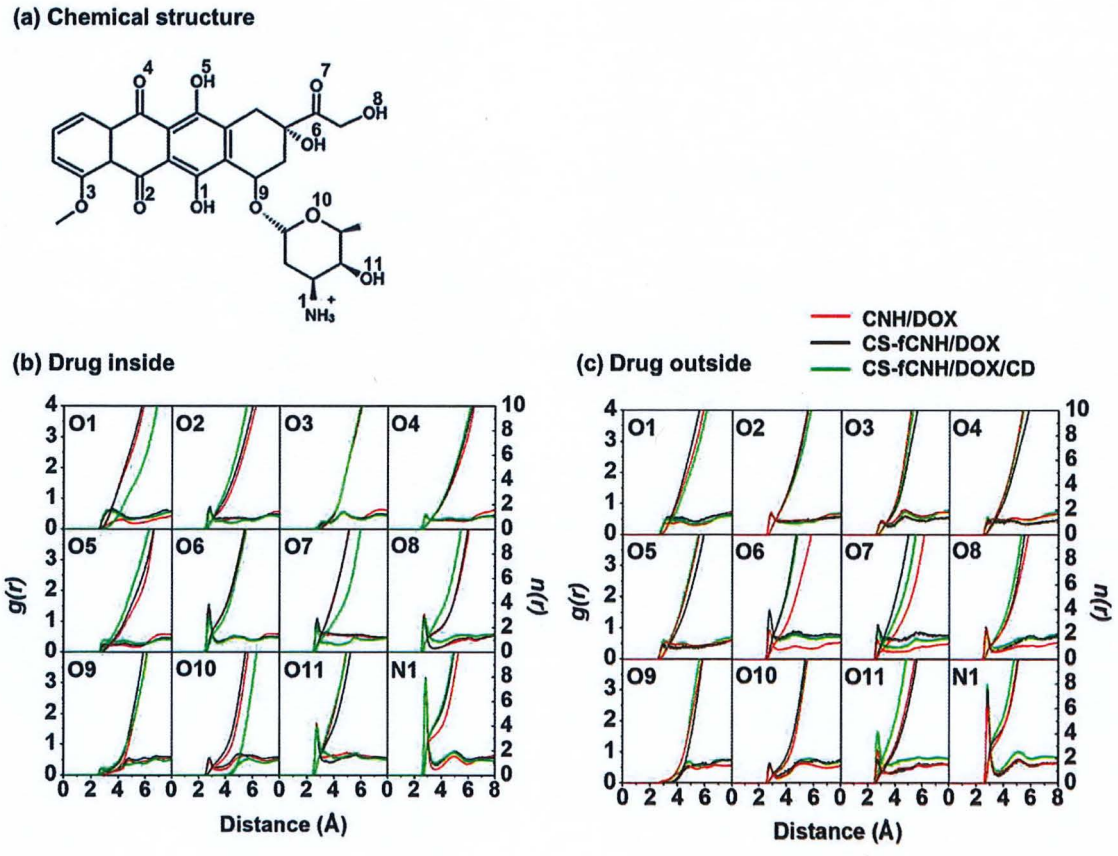

Figure 6. The RDFs of water molecules around the DOX inside (a) and DOX outside (b) of all system.

3.3 molecular Interaction

The number of atomic contacts within 3 Å around DOX structure in Figure 6 were plotted to describe the interaction of DOX in its vehicle. The black line was found high values in all DOX_{inside} system and $DOX_{outside}$ without CS system all of simulation time. For $DOX_{outside}$ on chitosan chain at start of simulation, the gray peaks showed the value higher than the value in CNH all of simulation time. However, in system CD-CS-f-CNH/$DOX_{outside}$ (A), the results are different with others. Its contact between $DOX_{outside}$ and CNH increased while that between $DOX_{outside}$ and CD-CS chain decreased after 350 ns of dynamic. The results suggest that DOX can occur molecular interaction between DOX and CNH and CD-CS chain. CD-CS-f-CNH/$DOX_{outside}$ (A) results indicated that the DOX can move from CD-CS to bind with CNH when there was large gap between a CS chain wrapped CNH.

The behavior of DOX with its vehicle were found by results of distance and number of contacts. Binding between The DOX and CNH prefers to bind around center of CNH both DOX inside and outsides CNH when CNH was wrapped with CS or CD-CS, the DOX inside can more move from center of CNH while DOX outside showed strong interaction between DOX and CS. However, DOX outside CNH can bind with CNH when the S-ring were twisted.

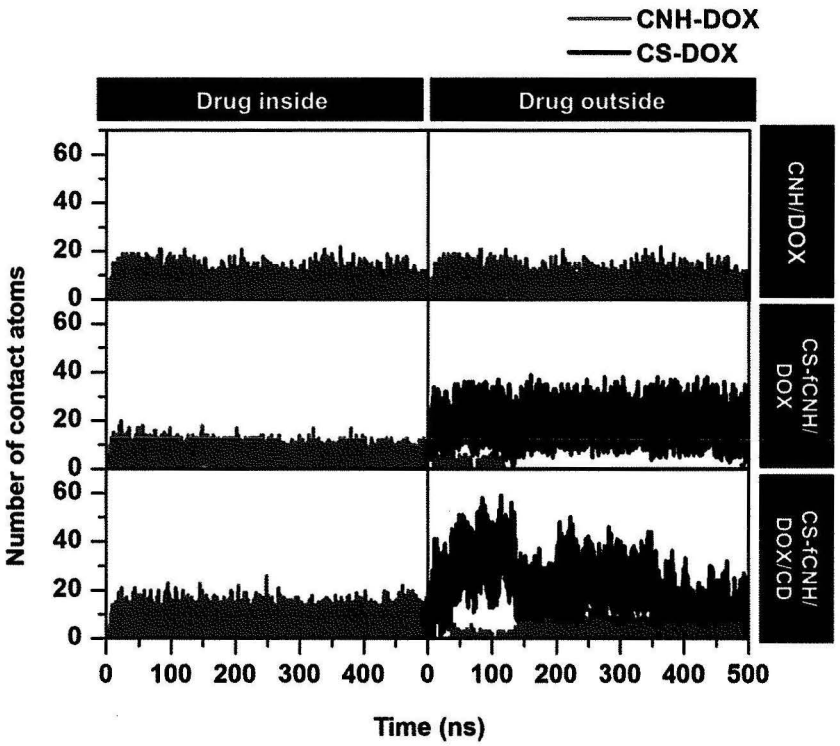

Figure 7. the plot of number of contact between $DOX_{inside/outside}$ and CNH (color), $DOX_{inside/outside}$ and CS (color), and $DOX_{inside/outside}$ and CD (color)

3.4 binding free energy of system

The binding between DOX and CNH, CS-fCHN/DOX and CS-fCHN/DOX/CD were calculated using MMPBSA and represented in Table 1 and 2. The VDW is lowest interaction energy for all systems. The results indicated that the main interaction between DOX and CNH and CS is VDW interaction. For ΔG, the results of the drug inside CNH presents the same value as well as the result in $DOX/CNH_{outside}$. ΔG between DOX and CNH surface are about -51 to -67 kcal/mol. the lowest ΔG is CS-fCHN/DOX_{inside}/CD while the ΔG values of drug outside are found around -15 to -23 kcal/mol. the results indicated that binding affinity between DOX and surface of CNH is stronger than binding affinity between DOX and CS chain. Furthermore, the CS chain wrapped

around CNH surface can enhance binding affinity of DOX within CNH by increasing of VDW interaction.

Table 1. The binding free energy of drug inside systems from MMPBSA (kcal/mol)

Drug inside	**VDW**	**EEL**	**ΔE_{gas}**	**ΔE_{solv}**	**ΔE_{total}**	**ΔG**
CHN/DOX	-60.69±0.04	-9.76±0.08	-70.45±0.09	27.30±0.10	-43.16±0.04	-53.53±0.04
CS-fCHN/DOX	-58.05±0.06	-1.49±0.02	-59.54±0.07	13.19±0.04	-46.35±0.04	-51.72±0.04
CS-fCHN/DOX/CD	-77.29±0.05	10.72±0.02	-66.57±0.05	5.27±0.03	-61.30±0.04	-67.26±0.04

Table 2. The binding free energy of drug outside systems from MMPBSA (kcal/mol)

Drug outside	**VDW**	**EEL**	**ΔE_{gas}**	**ΔE_{solv}**	**ΔE_{total}**	**ΔG**
CHN/DOX	-39.55±0.02	-4.89±0.04	-44.44±0.04	10.05±0.05	-34.38±0.02	-58.68±0.02
CS-fCHN/DOX	-29.50±0.03	-10.19±0.05	-39.69±0.07	25.74±0.05	-13.94±0.03	-14.91±0.03
CS-fCHN/DOX/CD	-38.62±0.07	-12.81±0.10	-51.43±0.10	29.58±0.10	-21.85±0.06	-23.68±0.06

Conclusions

Pristine CNH, CS-f-CHN and CS-f-CHN/DOX/CD have ability of drug carrier for DOX and the DOX within DMBCD present increasing of capacity of CS-f-CHN/DOX/CD system. the DOX within and without CNH surfaces can move and fluctuate between middle and Edge of CNH. However, The DOX on CS present stability at the initial residue of CS but $DOX_{outside}$ can move to bind with CNH surface. For salvation properties of DOX the drug inside and outside CNH are similar properties as well as results in CS-f-CHN and CS-f-CHN/DOX/CD system. the location and CS wrapped around surface of CNH no effect to DOX solubility. In addition, the binding affinity from contact atoms and MMPBSA results suggested that the binding affinity between DOX and CNH is stronger than DOX and CS chain. Whereas number of contact atom between DOX and CS are higher than that between DOX and CNH. The DOX can move from CS to bind with CNH. However, the CS chain can promote binding affinity of DOX inside CHN. This mean that CS can help the drug binding with CNH lead to increasing drug release by VDW interaction.

Acknowledgements

This research was supported by the Rachadaphiseksomphot Endowment Fund, Chulalongkorn University (CU-GR_62_11_23_05). N.K. thanks The Second Century Fund (C2F), Chulalongkorn University. We are thankful for computational resources supported by NSTDA Supercomputer Center (ThaiSC) for this research.

References

[1] World Health Organization. (2018). The top 10 causes of death. Retrieved from https://www.who.int/news-room/fact-sheets/detail/the-top-10-causes-of-death.

[2] Virani, et al. (2017). National and Subnational Population-Based Incidence of Cancer in Thailand: Assessing Cancers with the Highest Burdens. *Cancers*. Retrieved from https://webcache.googleusercontent.com/search?q=cache:7QqBP6s7MgUJ:https://www.mdpi.com/2072-6694/9/8/108/pdf+&cd=1&hl=th&ct=clnk&gl=th.

[3] Wikipedia contributors. (2019, April 22). Doxorubicin. In *Wikipedia, The Free Encyclopedia*. Retrieved 02:36, June 1, 2019, from https://en.wikipedia.org/w/index.php?title=Doxorubicin&oldid=893594672

[4] Rungnim, C., Rungrotmongkol, T., & Poo-Arporn, R. P. (2016). pH-controlled doxorubicin anticancer loading and release from carbon nanotube noncovalently modified by chitosan: MD simulations. *J Mol Graph Model,* 70, 70-76. Retrieved from https://www.ncbi.nlm.nih.gov/pubmed/27677150. doi:10.1016/j.jmgm.2016.09.011

[5] University of Iowa Hospitals & Clinics. Side effects of anti-cancer drugs. Retrieved from https://uihc.org/health-topics/side-effects-anti-cancer-drugs

[6] Mishra, N., Pant, P., Porwal, A., Jaiswal, J., Aquib Samad, M., & Tiwari, S. (2016). *Targeted Drug Delivery: A Review* (Vol. 6).

[7] Alavi, M., Karimi, N., & Safaei, M. (2017). Application of Various Types of Liposomes in Drug Delivery Systems. *Advanced pharmaceutical bulletin, 7*(1), 3-9. Retrieved from https://www.ncbi.nlm.nih.gov/pubmed/28507932.

[8] Samad, A., Sultana, Y., & Aqil, M. (2007). *Liposomal Drug Delivery Systems: An Update Review* (Vol. 4).

[9] Seifert, L., & Miller, G. (2017). Molecular Pathways: The Necrosome-A Target for Cancer Therapy. *Clinical cancer research : an official journal of the American Association for Cancer Research, 23*(5), 1132-1136. Retrieved from https://www.ncbi.nlm.nih.gov/pubmed/27932417.

[10] Vanden Berghe, T., Hassannia, B., & Vandenabeele, P. (2016). An outline of necrosome triggers. *Cellular and molecular life sciences : CMLS, 73*(11-12), 2137-2152. Retrieved from https://www.ncbi.nlm.nih.gov/pubmed/27052312.

[11] Ganta, S., Talekar, M., Singh, A., Coleman, T. P., & Amiji, M. M. (2014). Nanoemulsions in Translational Research—Opportunities and Challenges in Targeted Cancer Therapy. *AAPS PharmSciTech, 15*(3), 694-708. Retrieved from https://doi.org/10.1208/s12249-014-0088-9. doi:10.1208/s12249-014-0088-9

[12] Jaiswal, M., Dudhe, R., & Sharma, P. K. (2015). Nanoemulsion: an advanced mode of drug delivery system. *3 Biotech, 5*(2), 123-127. Retrieved from https://www.ncbi.nlm.nih.gov/pmc/articles/PMC4362737/. doi:10.1007/s13205-014-0214-0

[13] Carneiro, S. B., Costa Duarte, F. Í., Heimfarth, L., Siqueira Quintans, J. d. S., Quintans-Júnior, L. J., Veiga Júnior, V. F. d., & Neves de Lima, Á. A. (2019). Cyclodextrin¯Drug Inclusion Complexes: In Vivo and In Vitro Approaches. *International journal of molecular sciences, 20*(3), 642. Retrieved from https://www.ncbi.nlm.nih.gov/pmc/articles/PMC6387394/. doi:10.3390/ijms20030642

[14] Jacob, S., & Nair, A. (2018). *Cyclodextrin complexes: Perspective from drug delivery and formulation* (Vol. 79).

[15] Kothamasu, P., Kanumur, H., Ravur, N., Maddu, C., Parasuramrajam, R., & Thangavel, S. (2012). Nanocapsules: the weapons for novel drug delivery systems. *BioImpacts : BI, 2*(2), 71-81. Retrieved from https://www.ncbi.nlm.nih.gov/pmc/articles/PMC3648923/. doi:10.5681/bi.2012.011

[16] Lacoeuille, F., Garcion, E., Benoit, J.-P., & Lamprecht, A. (2008). *Lipid nanocapsules for intracellular drug delivery of anticancer drugs* (Vol. 7).

[17] Ahmad, Z., Shah, A., Siddiq, M., & Kraatz, H. (2014). *Polymeric micelles as drug delivery vehicles* (Vol. 4).

[18] Amin, M. C. I. M., Butt, A. M., Amjad, M. W., & Kesharwani, P. (2017). Chapter 5 - Polymeric Micelles for Drug Targeting and Delivery. In V. Mishra, P. Kesharwani, M. C. I. Mohd Amin, & A. Iyer (Eds.), *Nanotechnology-Based Approaches for Targeting and Delivery of Drugs and Genes* (pp. 167-202): Academic Press.

[19] De Jong, W. H., & Borm, P. J. A. (2008). Drug delivery and nanoparticles:applications and hazards. *International journal of nanomedicine, 3*(2), 133-149. Retrieved from https://www.ncbi.nlm.nih.gov/pubmed/18686775.

[20] Yan, L., & Chen, X. (2014). 7 - Nanomaterials for Drug Delivery. In S.-C. Tjong (Ed.), *Nanocrystalline Materials (Second Edition)* (pp. 221-268). Oxford: Elsevier.

[21] Tiwari, G., Tiwari, R., Sriwastawa, B., Bhati, L., Pandey, S., Pandey, P., & Bannerjee, S. K. (2012). Drug delivery systems: An updated review. *International journal of pharmaceutical investigation, 2*(1), 2-11. Retrieved from https://www.ncbi.nlm.nih.gov/pmc/articles/PMC3465154/. doi:10.4103/2230-973X.96920

[22] Zhang, W., Zhang, Z., & Zhang, Y. (2011). The application of carbon nanotubes in target drug delivery systems for cancer therapies. *Nanoscale research letters, 6*(1), 555-555. Retrieved from https://www.ncbi.nlm.nih.gov/pmc/articles/PMC3210734/. doi:10.1186/1556-276X-6-555

[23] Hawelek, L., Schiavon, M., Szade, J., Wlodarczyk, P., Jurkiewicz, K., Fischer, H. E., . . . Burian, A. (2017). The atomic scale structure of dahlia-like single wall carbon nanohorns

produced by direct vaporization of graphite. *Diamond and Related Materials, 72*, 26-31. Retrieved from http://www.sciencedirect.com/science/article/pii/S0925963516302126. doi:https://doi.org/10.1016/j.diamond.2016.12.015

[24] Challa, R., Ahuja, A., Ali, J., & Khar, R. K. (2005). Cyclodextrins in drug delivery: an updated review. *AAPS PharmSciTech, 6*(2), E329-E357. Retrieved from https://www.ncbi.nlm.nih.gov/pmc/articles/PMC2750546/. doi:10.1208/pt060243

[25] Matioli, G., Zanin, G., F. Gljimarães, M., & Moraes, F. (1998). *Production and Purification of CGTase of Alkalophylic Bacillus Isolated from Brazilian Soil* (Vol. 70-72).

[26] hoi, S. G., Lee, S.-E., Kang, B.-S., Ng, C. L., Davaa, E., & Park, J.-S. (2014). Thermosensitive and mucoadhesive sol-gel composites of paclitaxel/dimethyl-β-cyclodextrin for buccal delivery. *PloS one, 9*(9), e109090-e109090. Retrieved from https://www.ncbi.nlm.nih.gov/pmc/articles/PMC4183572/. doi:10.1371/journal.pone.0109090

[27] Li, N., Zhao, Q., Shu, C., Ma, X., Li, R., Shen, H., & Zhong, W. (2015). Targeted killing of cancer cells in vivo and in vitro with IGF-IR antibody-directed carbon nanohorns based drug delivery. *International Journal of Pharmaceutics, 478*(2), 644-654. Retrieved from http://www.sciencedirect.com/science/article/pii/S0378517314009120. doi:https://doi.org/10.1016/j.ijpharm.2014.12.015

[28] Karnati, K. R., & Wang, Y. (2018). Understanding the co-loading and releasing of doxorubicin and paclitaxel using chitosan functionalized single-walled carbon nanotubes by molecular dynamics simulations. *Physical chemistry chemical physics : PCCP, 20*(14), 9389-9400. Retrieved from https://www.ncbi.nlm.nih.gov/pmc/articles/PMC5898243/. doi:10.1039/C8CP00124C

[29] Duan, Y., Wu, C., Chowdhury, S., C Lee, M., Xiong, G., Zhang, W., . . . Kollman, P. (2003). *A Point-Charge Force Field for Molecular Mechanics Simulations of Proteins Based on Condensed-Phase Quantum Mechanical Calculations* (Vol. 24).

[30] Tessier, M. B., Demarco, M. L., Yongye, A. B., & Woods, R. J. (2008). Extension of the GLYCAM06 Biomolecular Force Field to Lipids, Lipid Bilayers and Glycolipids. *Molecular*

406 *simulation, 34*(4), 349-363. Retrieved from
407 https://www.ncbi.nlm.nih.gov/pmc/articles/PMC3256582/.
408 doi:10.1080/08927020701710890

409 [31] Elber, R., Ruymgaart, A. P., & Hess, B. (2011). SHAKE parallelization. *The European physical*
410 *journal. Special topics, 200*(1), 211-223. Retrieved from
411 https://www.ncbi.nlm.nih.gov/pmc/articles/PMC3285512/. doi:10.1140/epjst/e2011-
412 01525-9

413 [32] Cheatham, T. E., III, Miller, J. L., Fox, T., Darden, T. A., & Kollman, P. A. (1995). Molecular
414 Dynamics Simulations on Solvated Biomolecular Systems: The Particle Mesh Ewald
415 Method Leads to Stable Trajectories of DNA, RNA, and Proteins. *Journal of the American*
416 *Chemical Society, 117*(14), 4193-4194. Retrieved from
417 https://doi.org/10.1021/ja00119a045. doi:10.1021/ja00119a045

418 [33] Genheden, S., & Ryde, U. (2015). The MM/PBSA and MM/GBSA methods to estimate ligand-
419 binding affinities. *Expert opinion on drug discovery, 10*(5), 449-461. Retrieved from
420 https://www.ncbi.nlm.nih.gov/pmc/articles/PMC4487606/.
421 doi:10.1517/17460441.2015.1032936

422 [34] Eduardo R. A. Leonardo A. De S. Wagner B. De A l. Hélio F.Dos S. (2019). Molecular dynamics
423 of carbon nanohorns and their complexes with cisplatin in aqueous solution, 89, 167-
424 177. Retrieved from https://doi.org/10.1016/j.jmgm.2019.03.015
425
426